2015

PERSISTENT ORGANIC POLLUTANTS IN THE ARCTIC, ATLANTIC AND PACIFIC OCEANS

Caoxin Sun
University of Rhode Island, caoxin@my.uri.edu

PERSISTENT ORGANIC POLLUTANTS IN THE ARCTIC, ATLANTIC AND PACIFIC OCEANS

BY

CAOXIN SUN

A THESIS SUBMITTED IN PARTIAL FULFILLMENT OF THE

REQUIREMENTS FOR THE DEGREE OF

MASTER OF SCIENCE

IN

OCEANOGRAPHY

UNIVERSITY OF RHODE ISLAND

2015

MASTER OF SCIENCE THESIS

OF

CAOXIN SUN

APPROVED:

Thesis Committee:

Major Professor Rainer Lohmann

Brice Loose

Gavino Puggioni

Nasser H. Zawia
DEAN OF THE GRADUATE SCHOOL

UNIVERSITY OF RHODE ISLAND
2015

ABSTRACT

Persistent organic pollutants (POPs) are a group of compounds that are persistent, toxic, bioaccumulative and undergo long range transport. Polychlorinated biphenyls (PCBs), organochlorine pesticides (OCPs) and polybrominated diphenyl ethers (PBDEs) are three groups of POPs. They were widely used as dielectric and coolants fluids, pesticides and flame retardants, respectively. Polycyclic aromatic hydrocarbons (PAHs), normally produced by incomplete combustion of carbonaceous materials, were not in the list but have similar properties as POPs. Even though restrictions and bans over POPs started decades ago (PCBs and OCPs in the 1970s and BDEs in the 2000s), POPs are still detected in the environment and could negatively affect human and wildlife health. Previous studies of POPs monitoring were mostly focused on land or coastal areas; POPs data in remote oceans are lacking. In this study, polyethylene passive samplers (PEs) were used for measuring POPs in the Atlantic and Pacific. The Atlantic study involved deep ocean measurements, while the Pacific study used surface seawater and atmosphere measurements. Deep ocean measurements were conducted by deep moorings at two locations, in the North and Tropical Atlantic Ocean. Results revealed the presence of POPs in the deep ocean with concentrations up to 10 pg L^{-1} for PCBs, OCPs and BDEs. Oceanic current study suggested that the concentration maximum around 800 m at the Tropical Atlantic site could be potentially originated from the Mediterranean Sea. Mass balance calculation indicated that deep ocean is an important storage for POPs (4.8-26 % of the global HCB environmental burdens). The Pacific study measured both gas-phase and dissolved phase POPs in the Pacific. Atmospheric and oceanic concentrations of PCBs were

detected at the magnitude of 1 pg m^{-3} and 0.1 pg L^{-1} respectively, except for PCB-8 which was detected at concentrations 10 times higher. HCB dominated in the gas phase (~300 pg m^{-3}), while α -HCH dominated in the dissolved phase (~100 pg L^{-1}). Large variations of BDEs and PAHs concentrations in either phase were found and were higher than most reported values. Close to equilibrium state of PCBs and OCPs were found in the oligotrophic Pacific. Absolute air-water exchange fluxes were <0.4 ng m^{-2} day^{-1} for PCBs and <4.5 ng m^{-2} day^{-1} for OCPs. Net air-water exchange gradients strongly favored gas-phase deposition of PBDEs into the water, while mixed gradients were found for PAHs.

ACKNOWLEDGMENTS

I would like to thank Dr. Rainer Lohmann for his guidance and expertise throughout this research. Also many thanks to everyone in the Lohmann lab for all peer-support. This work could not have been done without funding, which was largely provided by NSF.

PREFACE

This preface is included with the explicit intention to note that Manuscript Format has been used in the preparation of this thesis.

TABLE OF CONTENTS

LIST OF TABLES

LIST OF FIGURES

Vertical distribution of different POPs in North and Tropical Atlantic Ocean

Manuscript in preparation for submission to *Environmental Science and Technology*

Caoxin Sun[1], Thomas Soltwedel[2], Eduard Bauerfeind[2], Dave Adelman[1] and Rainer Lohmann[1,*]

[1]Graduate School of Oceanography, University of Rhode Island, South Ferry Road, Narragansett, 02882 Rhode Island, United States

[2]Alfred-Wegener-Institut, Helmholtz-Zentrum für Polar- und Meeresforschung, Am Handelshafen 12, 27570 Bremerhaven, Germany

ABSTRACT

Little is known of the distribution of POPs in the deep ocean. Polyethylene passive samplers were used for the first times studying vertical distribution of truly dissolved concentration of POPs at two sites in the Atlantic Ocean. Samples were collected at five depths ranging 26-2535 m in the North and Tropical Atlantic separately, with a sampling time around one year. Samplers of different thickness were used for the purpose of determining the state of equilibrium. Comparable sampling rates were obtained from model derived results (5 and 4 L/day) and performance reference compounds derived results (8.7 and 4.9 L/day). Concentrations of POPs detected in the North Atlantic near the surface ($\sum$PCB: 0.84 pg L^{-1}, $\sum$OCP: 11.4 pg L^{-1}, $\sum$BDE: 0.45 pg L^{-1}, $\sum$PAHs: 148 pg L^{-1}) were similar to previous measurements. Complex distribution pattern along depth was found at sites; potential POPs sources from currents other than particle absorption and sinking was suggested. A possible origin of the depth profile maximum of POPs at the tropical Atlantic site near 800 m in depth was the Mediterranean Sea. The ration of PCB concentrations (PCB-28 excluded) between the two sites was supportive of latitudinal fractionation theory ($R^2 = 0.95$, $p < 0.05$), with more mobile compounds travelling further north than less mobile compounds. A mass balance estimation of HCB implied significant storage in the deep ocean compartment (4.8-26 % of the global HCB environmental burdens), contrasting traditional beliefs of POPs not reaching the deep ocean.

INTRODUCTION

Open ocean seawater measurements of persistent organic pollutants (POPs) are scarce due to the difficulties associated with the sampling procedure, contamination and costs of cruises (Gioia et al., 2013). Even scarcer are the data on POPs in the deep ocean, since most of the measurements of POPs in the open ocean were limited to surface seawater. Little is known of the role played by deep ocean compartments in containing POPs from the surface (Booij et al., 2014).

There are very few previous measurements of deep oceanic POPs: (1) PCBs and PAHs in deep waters in the North Atlantic (near the South-Western edge of the Porcupine Abyssal Plain and around Iceland) using active sampling (Schulz-Bull et al.,1988); (2) PCBs in the central Arctic Basins (Nansen, Amundsen, and Makarov) again relying on active sampling (Sobek & Gustafsson, 2014); (3) PCBs, PAHs, HCB and DDE at 0.1-5 km depth in the Irminger Sea, the Canary Basin and the Mozambique Channel relying on passive sampling (Booij et al., 2014). These studies revealed the existence of POPs in the deep ocean and the significance of deep ocean as a compartment for storing POPs.

The study by Booij et al (2014) was the first to use passive sampling (semipermeable membrane devices, SPMD) to study the POPs vertical distribution in the ocean. Even though active sampling has been traditionally used, it bears the disadvantage of extensive labor and extreme care of controlling blank levels (Booij et al., 2014). Polyethylene sheets (PEs) is one common form of passive sampling devices. It has many advantages compared to other forms of passive samplers, such as simplicity in chemical makeup, low cost, easy handling and a high enrichment of POPs (Lohmann, 2012a). Passive sampling

was recently suggested a useful tool used monitoring POPs in open ocean (Lohmann & Muir, 2010).

Under the circumstances that the time to reach equilibrium is not known, the sampling rate (R_s) can be used to derive the state of equilibrium upon retrieval. One way to calibrate R_s is to use performance reference compounds (PRCs). PRCs are chemicals that are artificially made which share similar properties to target compounds. However, due to the extensive long time of pre-spiking samplers with PRCs, another approach has also been suggested by Bartkow et al. (2004) using different thickness to confirm that equilibrium has been reached.

In this study, polyethylene passive samplers of different thickness were deployed at two deep ocean sites (eastern Fram Strait and tropical Atlantic) in the Atlantic Ocean to determine vertical distributions of truly dissolved concentrations of several classes of POPs (Polychlorinated biphenyls (PCBs), organochlorine pesticides (OCPs), polybrominated diphenyl ethers (PBDEs) and polycyclic aromatic hydrocarbons (PAHs)). Concentrations derived from this study were compared to previous measurements to validate the reliability of using polyethylene passive samplers. The objectives of this study were to (i) assess the potential of using PEs for monitoring POPs in remote ocean; (ii) contrast various approaches to derive R_s (iii) contrast north-south and surface-to-deep gradients and (iv) improve the knowledge of fate and transport of POPs to the deep ocean.

METHODS

Sampling

PE Sheet Samplers Preparation

Polyethylene samplers were cut from commercial sheeting (United Plastics, Inc., Mount Airy, NC) with a thickness of 800 μm and 1600 μm, yielding 6 x 30 cm and 6 x 15 cm strips respectively of ~14 g each. For the tropical Atlantic deployment, two additional polyethylene samplers with a thickness of 50 μm were cut, yielding 10 x 30 cm stripes weighing ~2 g. All the PEs with a thickness of 800 μm and 1600 μm were precleaned in ethyl acetate for 10 days and then in *n*-hexane for 21 days. PEs with a thickness of 50 μm were prepared in by dichloromethane and *n*-hexane for 24 hrs each. These samplers were spiked with performance reference compounds (PRCs) accounting for percentage of loss during sampling. PRCs were spiked by immersing the samplers in 80:20 (v/v) methanol/water solutions for four weeks (Booij, Smedes, & Van Weerlee, 2002). Spiked PRCs include d_8-naphthalene, d_{10}-pyrene, d_{12}-benzo(a)pyrene, polybrominated biphenyls 9, 52, 103, and octachloronaphthalene.

Deep Mooring Sampling

Samplers were strung on stainless steel wires and attached to stainless porous cages. Cages were attached to deep mooring systems and deployed in North Atlantic (79˚ N, 4˚ E) and Tropical Atlantic (25˚ N, 38˚ W) separately (Figure 1.1). Deployment depths were 213 m, 468 m, 1173 m, 1736 m and 2535 m for the North Atlantic and 26 m, 84 m, 251 m, 800 m and 1800 m for the tropical Atlantic Ocean, respectively. Sampling time was around one year for both deployments (North Atlantic: July 21st 2012 ~ July 8th 2013; Tropical Atlantic: Sep 14th 2012 ~ Oct 1st 2013). Current velocities were also measured

during the two cruises. After samples were collected, they were wrapped in clean aluminium foil, shipped back to lab and stored at -4˚C until analysis.

Sample Analysis

Sample extraction

PEs were wiped clean using Kimwipes with Milli-Q water (Millipore, Billerica, MA). PEs were then cut into pieces (1 inch in length and width) and extracted in hexane overnight twice. 20 ng of surrogates ($^{13}C_{12}$-CB8, $^{13}C_{12}$-CB28, $^{13}C_{12}$-CB52, $^{13}C_{12}$-CB118, $^{13}C_{12}$-CB138, $^{13}C_{12}$-CB180, $^{13}C_{12}$-CB209; $^{13}C_{12}$-*p,p'*-DDT, $^{13}C_6$-HCBz; $^{13}C_{12}$-BDE28, $^{13}C_{12}$-BDE47, $^{13}C_{12}$-BDE99, $^{13}C_{12}$-BDE153, $^{13}C_{12}$-BDE183; d_{10}-acenaphthene, d_{10}-phenanthrene, d_{12}-chrysene, d_{12}-perylene) were spiked into the solution by syringe. After extraction, PEs were air dried and weighted. Extracts were combined in Turbovap tubes and concentrated to 1 ml under the condition of 30 ˚C water bath and 5 psi nitrogen blow. 1 ml extracts were then transferred into amber auto sampler GC-vials with another 2 ml rinse of Turbovap tubes in hexane. Extracts were further blown down to 100 μl by minivap and transferred into spring-bottom glass inserts with a 100 μl hexane rinse of GC-vials. 50 ng of injection standard (*p*-terphenyl-d_{14} and polybrominated biphenyl 30) was spiked into the final extracts for instrument analysis.

Instrumental Analysis

PCBs, OCPs and PBDEs were analyzed on a 6890N GC (Agilent, USA) - Quattro Micro tandem MS (Waters, Micromass, UK) on a DB5-MS fused silica capillary column (30 m $\times$0.25 mm, J&W Scientific). Injection was splitless 1 μL at 320 ˚C with Helium as

carrier gas at 1 mL min^{-1}. PCBs and OCPs were analyzed together during the same GC temperature program: 100 ˚C, hold 1 min, 8 ˚C/min to 180 ˚C, 3 ˚C/min to 260 ˚C, 10 ˚C/min to 300 ˚C, and hold for 6 min; PBDEs were run using: 100 ˚C, hold 3 min, 5 ˚C/min to 315 ˚C, and hold for 5 min . PAHs were analyzed on an Agilent 6890 Series GC - Agilent 5973 Network MS Detector on a DB-6 MS fused silica capillary column (30 m × 0.25 mm, J&W Scientific). Injection was splitless 1 μL at 280 ˚C with Helium as carrier gas at 1 mL min^{-1}. GC temperature program was: 90 ˚C, hold 3 min, 5 ˚C/min to 110 ˚C, 8 ˚C/min to 200 ˚C, 5 ˚C/min to 315 ˚C, and hold for 5 min.

Quality assurance/Quality control

Matrix spike and lab blanks were performed for each batch of approximately 10 samples. Field blanks were taken during the North Atlantic deployment. All blanks were extracted in the same method as samples. Limits of detection (LOD) were derived from field blanks and determined by three times the standard deviation of field blank samples. Detailed QA/QC information on detection limits are in the supporting information.

PE concentration (C_{PE}) **conversion to environmental concentration**

Concentration of target compounds in the PEs (C_{PE}, ng g^{-1}) were converted to concentration freely dissolved in water (C_w, kg L^{-1}) by equation (1)

$$C_w = \frac{C_{PE}}{K_{PEw}} \times \frac{1}{\%\text{equilibrium}} \quad (1)$$

where K_{PEw} is the compound specific partitioning coefficient between PE and water (L kg^{-1}) whose temperature correction for K_{PEw} was done using equation (2) and

%equilibrium is the percentage of equilibrium achieved by individual compound in the sampling period which is given by equation (3)

$$K_{\mathrm{PEw}}\ (T) = K_{\mathrm{PEw}}\ (298)\ \mathrm{e}^{(\Delta H_{\mathrm{PEw}}/\mathrm{R})\ \{\frac{1}{298}-\frac{1}{T}\}} \quad (2)$$

where $K_{\mathrm{PEw}}(T)$ and $K_{\mathrm{PEw}}(298)$ are PEw partitioning coefficients at temperature T (K) and 298 K, respectively;

ΔH_{PEw} is the enthalpy of PEw partitioning (kJ mol^{-1}); and

R is the universal gas constant (8.3143 J mol^{-1} K^{-1});

$$\%\mathrm{equilibrium} = 1\ -\ \mathrm{e}^{(\frac{-R_s t}{K_{\mathrm{PEw}}\ V_{\mathrm{PE}}})} \quad (3)$$

where R_s is the sampling rate (L/day) for one whole sampling sheet;

t is sampling time (days); and

V_{PE} is the volume of the PE (L).

Estimation of sampling rate

Using Different Thickness

Sampling rates were estimated based on the assumption that PEs deployed at the same depth/cage were exposed to the same truly dissolved concentration (C_w), and that the same sampling rate applies to all compounds. R_s pairs were assumed to be from different combinations of integers from 1~X L/day (X=100, 50, 40, 30 20, 10). For each combination, %equilibrium was calculated using equation (6) and the environmental concentration was further determined using equation (1). The aim was to find the exact pair of R_s that minimizes the total of standard deviations of all detected compounds. The total of standard deviations is defined as

$$\sum_{i=1}^{n} s_i \tag{4}$$

where n is the number of pairs of data,

s is the standard deviation of the derived environmental concentration (x_j) by the two PEs in the same cage

$$s = \sqrt{\frac{1}{N-1}\sum_{j=1}^{N}(x_j - \bar{x})^2} \qquad (N=2) \tag{5}$$

Using PRCs

Site specific sampling rates were also calculated via a nonlinear least-squares method adapted from (Booij & Smedes, 2010). This method only applies to PEs that were pre spiked with PRCs, i.e., 50 μm thick ones for tropical Atlantic deployment.

Estimation of water age using CFCs

Transient tracers, including CFCs are useful as a water mass tracer because their atmospheric concentration can be uniquely related to a calendar year. In turn, water at the ocean surface records this unique concentration based upon air-water gas partitioning. The equilibrium partitioning between CFC concentration in the air and water is described by Henry's Law. Dissolved CFCs concentration C_w (mol kg^{-1}) in the interested locations were obtained from CLIVAR and Carbon Hydrographic Data Office (CCHDO). Temperature and salinity data were obtained from the same origin and were used for deriving the Henry's Law Constant H (mol kg^{-1}). The molar ratio of CFCs in the atmosphere χ (mol CFC mol^{-1} air) were then calculated using

$$\chi = \frac{C_w}{H} \tag{6}$$

χ data were from CDIAC (Bullister, 2014). SF_6 data were of the highest priority if available; if not, CFC-12 data were used instead.

RESULTS AND DISCUSSION

Equilibration of target analytes during Deployments

Passive samplers of different thickness were deployed to gauge the equilibration of target compounds during deployments. Obtaining similar (mass- normalized) concentrations of target analytes would indicate equilibrium had been attained during the field deployments. Yet the deployment times (1 year each) were not long enough to reach equilibrium for most target analytes, hence we relied on other approaches to deduce truly dissolved concentrations of target compounds in the Atlantic Ocean. PRC derived sampling rate (4.9 and 8.7 L/day) at two depths indicated the necessity to deduce site- and depth-specific sampling rates for each deployment.

Estimating Sampling Rate and state of Equilibrium

Sampling rates were obtained by the modeling approach mentioned above. From previous observations, Rs are typically in the range of 1~100 L day^{-1}. Scenarios (1) to (6) (with upper limits for the model-fit X=100, 50, 40, 30, 20, 15 L day^{-1}) were run and interpreted (Figure S1 & S2, Supporting Information). In our deployments, 800 µm PEs had twice as large surface area as 1600 µm PEs; and Rs is proportional to surface area at linear uptake stage. The ratio POP's concentrations from the 800 µm PEs to 1600 µm PEs should be 2:1 if both were at linear uptake stage and closer to 1:1 if 800 µm PEs were at curvy linear uptake stage.

For the Tropical Atlantic deployments, it can be seen that the averaged ratio of Rs between PEs of two thickness were all 1.8 for six scenarios, implying that compounds in the 800 μm PEs already went beyond the linear uptake stage. For North Atlantic, Rs ratios were closest to 2 under scenario (6) (Table S6). For this reason, Rs range between 1~10 L/day was chosen for the North Atlantic. Additionally, current and deployment conditions in the North Atlantic were similar as in the Tropical Atlantic (shown as the measured current speed in Figure S1 & S2) and thus large variations of Rs were not expected between these two sites. The same Rs range (1~10 L/day) was chosen for the Tropical Atlantic.

The PRC derived Rs were 8.7 and 4.9 for 84 m and 251 m at depth which were less than the variance of currents between these two depths, indicating that deployment cages effectively buffered samplers from current velocity. This limiting factor can also be shown in Table S5 that no strong and significant positive correlations of Rs with current can be found in either scenario. Given the small range of current speed at the five sampling depths and the current limiting factor from the deployment cages, scenarios (6) were selected. Comparison of the result of the scenario (6) with PRC derived Rs were shown in Table 1.1 suggests good agreement between these two methods. Rs changes within a factor of 2 only gives difference in final concentration (North Atlantic PCBs) within a factor of 2, as shown in Table S7.

The percentage of equilibrium which target compounds achieved is shown in Table S8 and Table S9. Smaller sized compounds had fully reached equilibrium; the percentage of equilibrium reached decreases with increasing molecular weight. For the largest PCB congeners, less than 10% equilibrium had been achieved. For most OCPs, due to their

rather small size, more than 20% of equilibrium had been achieved by most compounds. PBDE congeners, on the other hand, all had attained only a low percentage of equilibrium. The large uncertainty associated with percentage of equilibrium for heavier compounds lead to large uncertainty with their derived truly dissolved concentrations. All concentrations discussed below are based on modeling results from scenario 6 (Rs = 1~10 L day^{-1}).

Truly dissolved surface concentrations of POPs

Tropical Atlantic

$\sum_{14}$PCBs concentrations near the surface of the tropical Atlantic were 8.5 pg L^{-1}, with $\sum_{ICES}$PCBs (PCB-28, 52, 90/101, 118, 138,153 and 180) of 6.2 pg L^{-1}; they constituted ~73% of all the $\sum_{14}$PCBs detected. $\sum_{14}$PCBs was close to the high end of reported value of ($\sum_{27}$PCBs , 0.24-5.7 pg L^{-1}) by Gioia et al. (2008b) but lower than the measurement ($\sum_{36}$PCBs North Atlantic, 26 pg L^{-1}) by Iwata et al. (1993). $\sum_{ICES}$PCBs was larger than (mean 2.5 pg L^{-1}) by Lohmann et al. (2012b) and (0.071-1.7 pg L^{-1}) by Gioia et al. (2008b).

HCB concentration was found at 6.0 pg L^{-1} near surface, higher than what was found in the North Atlantic (0.1-3 pg L^{-1}) by Lohmann et al. (2012b) but within the range of Northern Hemisphere average (2-9 pg L^{-1}) by Booij et al. (2007). *p,p'*-DDT, *o,p'*-DDT and *p,p'*-DDE were all within the range of 0.2-0.5 pg L^{-1}, which was in agreement with North Atlantic (0.1-3 pg L^{-1}) by Lohmann et al. (2012b) and close to the lower end of Northern Hemisphere average (0.3-1.4 pg L^{-1}) by Booij et al. (2007) and detected near 30˚N Atlantic (0.5 pg L^{-1}) by Iwata et al. (1993).

The only detectable PBDEs were 47, 100 and 99. Concentrations were 1.4, 0.3 and 1.6 pg L^{-1}, slightly higher than (~ 0.5 pg L^{-1} for 47 and around 0.1 pg L^{-1} for 99 and 100) by Lohmann et al. (2013a) and (0.02-1.05, nd-0.11 and 0.01-0.53 pg L^{-1} respectively) by Xie et al. (2011). In the first study, PEs were used for collecting samples; on the second cruise, XAD resins and GFF were used as active sampling. Nonetheless, results from all three studies were fairly similar to each other.

Detected $\sum_7$PAHs was 83 pg L^{-1} near surface; which is within the range of ($\sum_{10}$PAHs, 58-1070 pg L^{-1}) by Nizzetto et al. (2008) and lower than ($\sum_3$PAHs , average of 270 pg L^{-1}) by Lohmann et al. (2013b). The higher end of the previous range occurred near the northwest coast of Africa, which was potentially influenced by emerging oil industry, biomass burning and natural source of PAHs in Africa. Therefore the unexpected large numbers (0.7-1 ng L^{-1}) were not representative of remote ocean concentrations in tropical Atlantic. The second study was near the coast of America thus detected ∑PAHs were not comparable to remote ocean, either. As to individual PAHs, phenanthrene, fluroanthrene and pyrene were dominant, which is in agreement with (Nizzetto et al., 2008) and (Lohmann et al., 2013b).

Taken together, the concentrations of various POPs near the surface of the tropical Atlantic were in agreement with previous measurements reported for the remote Atlantic.

North Atlantic

In the North Atlantic, surface ∑PCBs concentration of the dissolved phase was 0.8 pg L^{-1} in this study, which was comparable to what was observed for $\sum_7$PCBs (0.7 pg L^{-1}) (Sobek & Gustafsson, 2014), $\sum_6$PCBs (< 1 pg L^{-1}) (Gioia et al., 2008a). As for

individual congeners, the highest concentration was determined by PCB-28, followed by 18, 44, 52 and then 101, 138, 153. This result is in agreement with result from Gioia et al. (2008a). PCB-18, 28, 52, 101, 118, 138, 153 were the most detected congeners in previous studies; they were also present in this study.

Hexachlorobenzene (HCB) was the OCP detected at the highest concentration. The near surface concentration was 10 pg L^{-1}, higher than those reported for NABE (0.1-0.8 pg L^{-1}) (Zhang et al., 2012) but close to results from the ARKXX cruise (high Arctic , 4-10 pg L^{-1}) (Lohmann et al., 2009), results for the East Atlantic Ocean (2-9 pg L^{-1}) (Booij et al., 2007) and for the Arctic Ocean (7 pg L^{-1}) (Strachan et al., 2000). It was mentioned by Lohmann et al. (2009) that $[HCB]_{diss}$ was negatively correlated with water temperature (T_w): $[HCB]_{diss} = 6.4\text{-}0.57 \times T_w$. Considering the higher averaged temperature from the NABE study (10 °C), $[HCB]_{diss}$ was close to the other reported values after temperature corrections.

There was no HCH detected, due to the less hydrophobic nature of HCHs which reduced their uptake by PEs. *p,p'*-DDE and *p,p'*-DDD are two breakdown products of *p,p'*-DDT. Their concentrations were around 0.1-0.4 pg L^{-1}, which were also close to previous studies (Lohmann et al., 2009; Zhang et al., 2012) . *p,p'*-DDT concentration was lower than *p,p'*-DDE and *p,p'*-DDD, indicating that there is no new source of *p,p'*-DDT to the central Arctic Basin.

The only PBDEs detected were BDE-99 and BDE-100. Surface seawater concentrations in the dissolved phase were 0.4 pg L^{-1} and 0.025 pg L^{-1}, respectively. Concentrations were similar to those observed in the Asian Arctic by Möller et al. (2011a) and East Greenland

Sea by Möller et al. (2011b). While BDE-47 was one of the dominant PBDEs in the other studies, it was not detected in this study in the Arctic.

∑PAHs was 148 pg L^{-1}, higher than (16-65 pg L^{-1}) by Schulz-Bull et al. (1998). Fluoranthene was detected with the highest concentration among all PAHs. Concentration of fluoranthene at 213 m (94 pg L^{-1}) fell in the range of other studies (Lohmann et al., 2009; Booij et al., 2014) in the similar area. There was no significant gradient of concentration with latitude. The ratio of fluoranthene over fluoranthene and pyrene ranged between 0.6 and 0.8. Lohmann et al. (2009) reported this ratio of 0.9-1.0 for the North Atlantic and Arctic Ocean; Schulz-Bull et al. (1998) reported 0.6 for the surface water of surface water in Irminger Sea. All these results suggested a combustion origin for the PAHs in the North Atlantic/Arctic region.

In summary, the concentrations of various POPs near the surface of the North Atlantic Ocean were in agreement with previous measurements reported for the remote Atlantic. Overall, this validates the use of PE samplers and the derived concentrations.

Certainty of derived truly dissolved concentrations

We compared how the use of different Rs (PRC-approach versus model-derived) affected truly dissolved concentrations of POPs. Maximum differences of 19% and 7% in equilibrium for PCBs were obtained (equilibrium using PRCs versus the equilibrium using modeling). PCBs cover a wide range of properties and are thus representative of the other compounds. Therefore, uncertainties associated with R_s were within a factor of 2 at most. The absolute concentrations of each individual compound between two PEs in one cage were also compared. The relative standard deviation of each detected compound

was calculated (Table S10). For North Atlantic samples, averaged relative standard deviation between two PEs from one cage at the same depth varied between 35-61 %; for tropical Atlantic samples, this range was 27-68 %. Variation was largely associated with the different detection limits between PEs of different thickness. The surface area of 800 μm PEs were twice as much as 1600 μm PEs, resulting in a faster uptake (Bartkow et al., 2004) and more contaminants above detection limits. Similarly, the surface area of 800 μm PEs and 50 μm PEs were the same, while the former one weighed 6~7 times more than the latter. Not surprisingly, more contaminants were above detection limits for 800 μm PEs than for the 50 μm PEs. The deviation of POP concentrations between 800 μm PEs and 50 μm PEs were, on average, larger (61 ± 9 %) than between 800 μm PEs and 1600 μm PEs (45± 12 %). For a better consistency between two sites as well as more detected compounds, only results from 800 μm PEs were used for Figure 1.2 and Figure 1.3 and all the other discussions of this chapter. This results in uncertainties of concentrations around a factor of 2, dominated by analytical uncertainty rather than sampling rate approaches.

Latitudinal Fractionation

The ratio of the concentration of each individual compound near the surface layer (231 m) at 79˚ N divided by the surface concentration at 24˚ N (26 m) was plotted as a function of their log vapor pressure (P_L) (Figure 1.5). The overall correlation was not strong ($R^2 = 0.25$), due to an outlier (PCB-28). Outlier was defined as values outside of 1.5 times of interquartile distance (IQD = Q3-Q1) subtracted from or added to the first quartile (Q1) and the third quartile (Q3) (Tukey, 1977). Similarly, an increasing trend of

concentration ratios of PCBs (88˚ N : 62˚ N) along with log vapor pressure was found by Sobek & Gustafsson. (2004). A significant higher concentration of PCB-28 in the north could be resulted from an unknown emission source near the sampling area. After removing PCB-28, the correlation between north-south ratio of POP concentrations and log P_L was much improved ($R^2 = 0.95$) and became significant ($p<0.05$). The results imply that higher mobility compounds (higher log P_L) display a relatively greater abundance up north than compounds with lower mobility. This supports the ideas formulated in the cold condensation theory. We note, however, that the two samples we used for the comparison were not real surface samples, especially for North Atlantic site. Therefore, the conclusions reached here have to be interpreted with caution, and are obviously affected by compounds not adhering to the trend.

Depth Profile (Tropical Atlantic Site)

Comparison with the other deep ocean POP measurements

Depth profiles were plotted as in Figure 1.2. The only comparable deep ocean measurements for the hexachlorobenzene (HCB) and fluoranthene (FLA) were measured at 1400 m depth in the Canary Basin near Northwest Africa by Booij et al. (2014), close to the 800 m concentrations from this study.

Depth profile shapes

PCBs, OCPs and PAHs congeners displayed similar depth profiles; mostly with a maximum at 800 m. Vertical profiles for PBDE are significantly different from the other compounds. All BDEs congeners exhibited a drastic decline in truly dissolved

concentrations below 251 m. Little BDEs were detected at depth, possibly linked to the fact that production of BDEs peaked 20~30 years later than those for PCBs and OCPs. Thus, PCBs and OCPs had more time to penetrate the deeper layers of the oceans, while PBDEs have only touched the surface ocean.

Explanations for depth profile

No measurements were done above 1400 m in the study of (Booij et al., 2014) and due to the similar concentrations found near the surface at other locations in the Atlantic, the authors concluded that no large concentration gradients existed in the upper 1400 m at Canary Basin. However, in the present study, a concentration maximum existed at 800 m which was significantly different from the other depths. We note that neither study was able to fully resolve depth profiles satisfactorily as only a few samplers were deployed, potentially missing important vertical features in POPs concentration.

Two hypotheses were tested to explain the shapes of the PCBs, OCPs and PAHs depth profiles: i) Particle binding/sinking; ii) Water current transport. Chemicals with higher K_{ow} (partitioning coefficient between octanol and water) tend to bind to particles more easily. With particles sinking and getting remineralized in the deep, POPs are released back into the water. PCBs, for instances, have different levels of chlorination and those with high chlorination degrees have higher tendency to bind to particles. The composition from different PCBs chlorination groups were plotted in Figure 1.4. There was little variation in the PCBs composition along with depth; the only noticeable trend is that penta- chlorinated PCBs decreased towards 250 m and a slight increase of tri- PCBs towards 1800 m. No trend of increasing contribution from higher chlorinated-PCBs was

shown, suggesting that particle binding/sinking process does not explain for the 800 m maximum.

The existence of Mediterranean water has been observed in East Atlantic (Martí et al. 2001). Mediterranean water sinks and mixes with Eastern Atlantic Water after it flows out of the Straits of Gibraltar, reaches equilibrium around 1000 m in depth and spreads across the North Atlantic (Knauss, 2005). So-called 'Meddies' are anticyclonic rings that were formed after Mediterranean water flows out of the Strait of Gilbraltar. They are 100 km in diameter and 800 m in thickness and could last as long as two or more years. It was estimated that some 25% of the Mediterranean outflow originates in Meddies and this makes meddies one tool to trace Mediterranean water. Meddies are normally associated with temperature and salinity anomalies, resulting from the warmer, saltier and younger feature of Mediterranean water. Fig S7 is the vertical section along East Atlantic. There is anomaly at 24.58˚N, 800 m in depth in all vertical profiles in Figure S4. CFC-11 data indicated a ring of younger water mass than surroundings. Although the longitude of the sampling location was not exactly as the CFC data, considering the size of meddies and the close proximity of these two locations, intruding from Mediterranean Water cannot be ruled out.

Another evidence towards the influence of Mediterranean Water on the sampler at 800 m in depth is the comparison to reported POPs in the Mediterranean Water. From the study conducted in 2006-2007, concentration in seawater were reported as $\sum_{41}$PCBs 2-84 pg L^{-1} and HCB up to 1.7 pg L^{-1} in the Mediterranean Sea and Black Sea (Berrojalbiz et al., 2011). The importance of penta- and hexa- chlorinated biphenyls were in agreement with tropical Atlantic samples reported here. Reported concentration of HCB in coastal water

of Alexandria, Egypt were much higher (27 pg L^{-1} surface and 12 pg L^{-1} subsurface) (AM, 1999).

The implication from our results is that the upper 1800 m of the water column was not well mixed and there were multiple water layers which potentially had different water mass origins, potentially affecting POPs concentrations and profiles.

Depth Profile (North Atlantic Site)

Depth Profile Shapes

Depth profiles were plotted as in Figure 1.3. All four groups of compounds showed similar depth profiles: a general decrease trend towards the deep and some maximum concentration appearing at 500 m in depth. Decreasing profiles of PCBs were observed in the 1990s in North Atlantic (Schulz-Bull et al., 1998; Schulz et al., 1988), while a nutrient-like profile was shown recently addressing the importance of advective flow-off from the continental shelf (Sobek & Gustafsson, 2014). The distribution pattern observed in this study neither follows a decreasing nor an increasing trend.

Explanations for depth profile

Similar to the discussion above, particle binding and sinking origination was tested by PCBs chlorination composition plotted in Figure 1.4. Compared to the results from the tropical Atlantic site, smaller degrees of chlorination tend to yield larger contribution of the ∑PCBs in the North Atlantic, which means the contribution from each group has the order of tri- > tetra- > penta- > hexa- . This composition pattern of chlorinated groups are in line with (Sobek & Gustafsson, 2014) and (Gioia et al., 2008a). No significant fraction

of higher chlorinated PCBs was observed along depth, indicating that particle sinking was not a major contributor to the PCBs in depth in North Atlantic either.

The Fram Strait is the pathway for water exchange between North Atlantic and Arctic Basin. Warm and saline eastern North Atlantic water flows into the Arctic Ocean in the eastern side of Fram Strait; cooled Arctic water flows out side of the basin in the west passage. At certain locations such as in Fram Strait between 77˚ and 77˚30'N; a significant part of Norwegian Atlantic Current (NwAC) converge does not enter the Arctic Ocean and directly recirculates south into the Nordic Seas(Schauer et al., 2004). The deep mooring site in this study was at a location that water flow in both directions occurs. From 1997 onwards, a deep oceanographic mooring array at 78˚50'N as well as three individual Hausgarten moorings were maintained in the Fram Strait. From the mooring data, it was noticed that deep water (~ 2500 m deep) in the plateau area near the Fram Strait Sill (~ 0˚ E) reflects mixing properties from two end members: the Greenland Sea Deep Water (GSDW) and the Eurasian Basin Deep Water (EBDW); at mooring site HC (Hausgarten Central), the water near bottom is almost purely EBDW. The mean flow at HC is locally topographically steered but does not achieve the cross sill advection (Appen et al., 2015). Unlike the Tropical Atlantic sampling site, it is hard to derive the water mass origins for certain depths at the North Atlantic sampling site due to the complexity and vigorousness in the water mixing processes.

CFCs ventilation ages and plots against PCBs profiles

Tropical Atlantic

There was no available SF_6 data for tropical Atlantic close to our deployment period; CFC-12 data were used instead to assess water mass origin and age. CFC-12 derived ventilation age was plotted against the ∑PCBs in Figure S3. Detailed information for ventilation age calculation was given in Table S11. The three sites chosen from CCHDO for the tropical Atlantic gave close CFC-12 data throughout the water column, indicating little variance of water composition around (24 ˚ N, 38 ˚ E). Ventilation age was then derived by averaging out the ventilation age from SITE1 to SITE 3 (Table S11). Concentration maximum of ∑PCBs had a ventilation age around 40 years, coinciding with the peak in PCBs emission in the 1970s. However, the ∑PCBs values near 800m are lacking, making it hard to determine whether 800 m ∑PCBs is the maximum throughout the whole water column. Meanwhile, it remains unknown how long the lag in the response time of oceanic POPs to global emission can be. Previous discussion talked about the potential influence from Mediterranean water on 800 m. Therefore, conclusion here is that ∑PCBs detected at the tropical Atlantic site generally followed the emission history of PCBs; it is unclear if the 800 m maximum reflected the 1970s PCBs emission peak.

North Atlantic

SF6 data was used for deriving the ventilation age of water masses in the North Atlantic. Large variations occurred between different sites chosen for the SF6 data, resulted from the complexity in bathymetric and water current conditions in this area. The closest sampling SF6 location to our PE sampling site which also covers the whole PE sampling depths was shown in Table S11. Figure S3 indicated a maximum in ∑PCBs at a

ventilation age of 10~20 years, younger than the maximum at tropical Atlantic site. Again, due to the limited data points, it is hard to accurately determine where the ∑PCBs maximum would occur. The whole distribution pattern of ∑PCBs with ventilation age still followed the global emission pattern, with one peak in the middle and decrease on both sides. The shift in the concentration peak of ~20 years could be an oceanic POPs response time lag not captured by the tropical Atlantic site measurement.

Mass balance Implications for POPs in the Ocean

For HCB, the vertical profiles reported here show no significant difference in absolute concentrations across the Atlantic Ocean. Therefore, we assumed a uniform spatial distribution across the Atlantic basin. Pilson estimated the whole surface area of Atlantic as 8.65×10^7 km^2 with average depth of 3,700 m (Pilson, 2013). The upper ocean (0-1,200 m) is loaded with HCB at a concentration of 9.6 ± 3.5 pg L^{-1} (mean ± standard deviation), while the deep ocean (1,200-3,700 m) has a concentration of 4.4 ± 1.6 pg L^{-1}, based on the results of this work. The total amount of HCB residing in the Atlantic Ocean is 1,947 ± 709 t; it accounted for 45 ± 16% of the total HCB stored in the ocean if using the estimation (4289 t) (Barber et al.,2005) . The total global production of HCB was estimated as >100,000 t by ATSDR (1997). The contemporary environmental burden of HCB was calculated as 10,000-26,000 t (Barber et al., 2005). Hence, the Atlantic Ocean stores less than 2.6 % of HCB ever produced, but contains 4.8-26 % of the global HCB environmental burdens.

IMPLICATION

Traditionally it is believed that the major inventory of POPs exist in the upper ocean only. However, this study supported previous work in highlighting the important role of deep ocean as a compartment storing POPs. Results from two contrasting sites also imply that the distribution of PCBs in the Oceans is influences by their mobility, with more mobile compounds being more abundant in the North rather than tropical Atlantic Ocean. The presence of numerous POPs in deeper water suggests that the deep ocean carries a significant mass already, particularly of the legacy POPs. As an example, PBDEs had penetrated the deep water masses of the Atlantic Ocean to a much smaller degree than the legacy PCBs and OCPs.

TABLES AND FIGURES

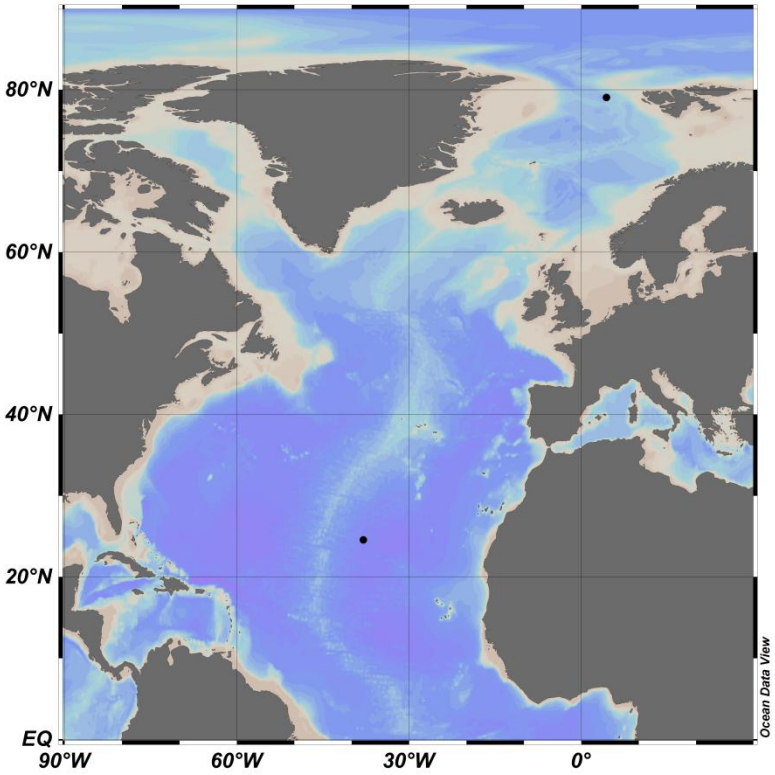

Figure 1.1 Sampling locations of the deep moorings.

Table 1.1 Comparison of Rs (L/day) derived by two methods (PRCs and modeling).

	PRCs	Modeling
84 m	8.7	5
800 m	4.9	4

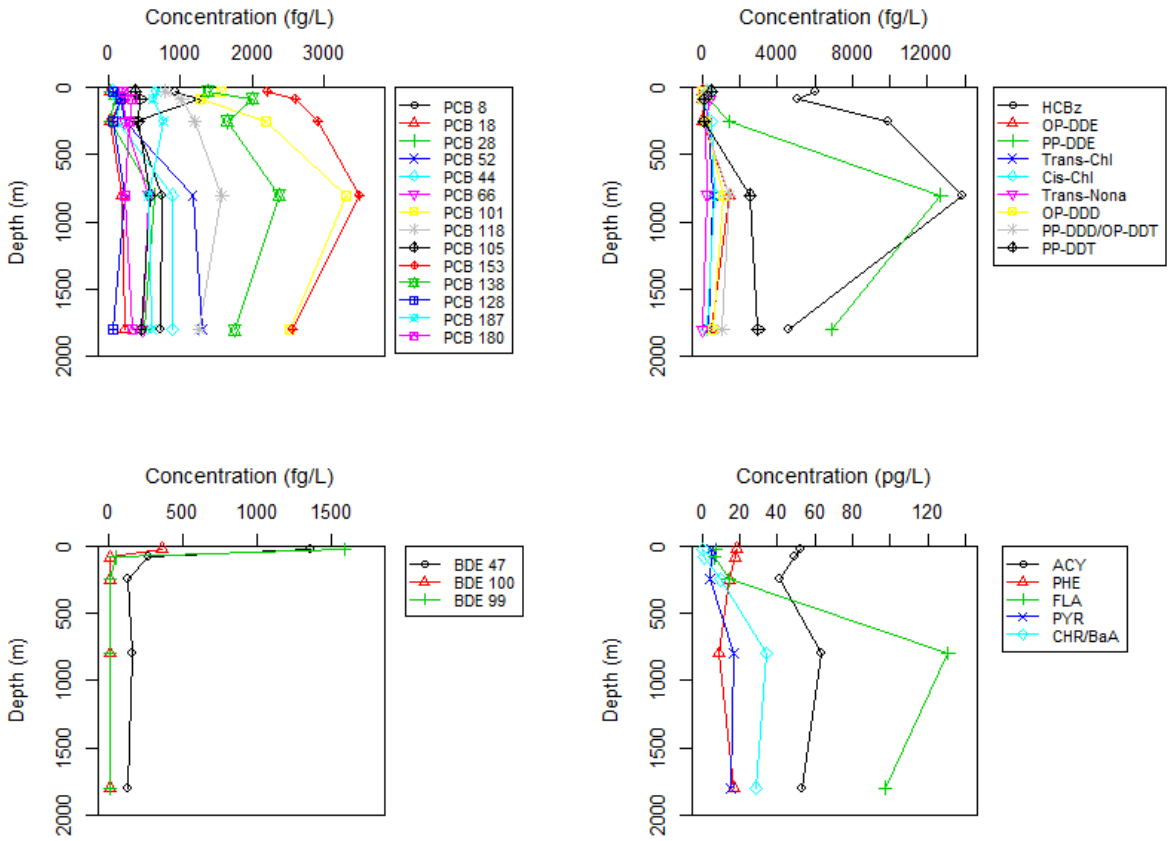

Figure 1.2 Depth profiles of POPs (PCBs, OCPs, PBDEs and PAHs) in the tropical Atlantic. Lines are for connecting points only and do not represent any measurements. This applies for the whole manuscript.

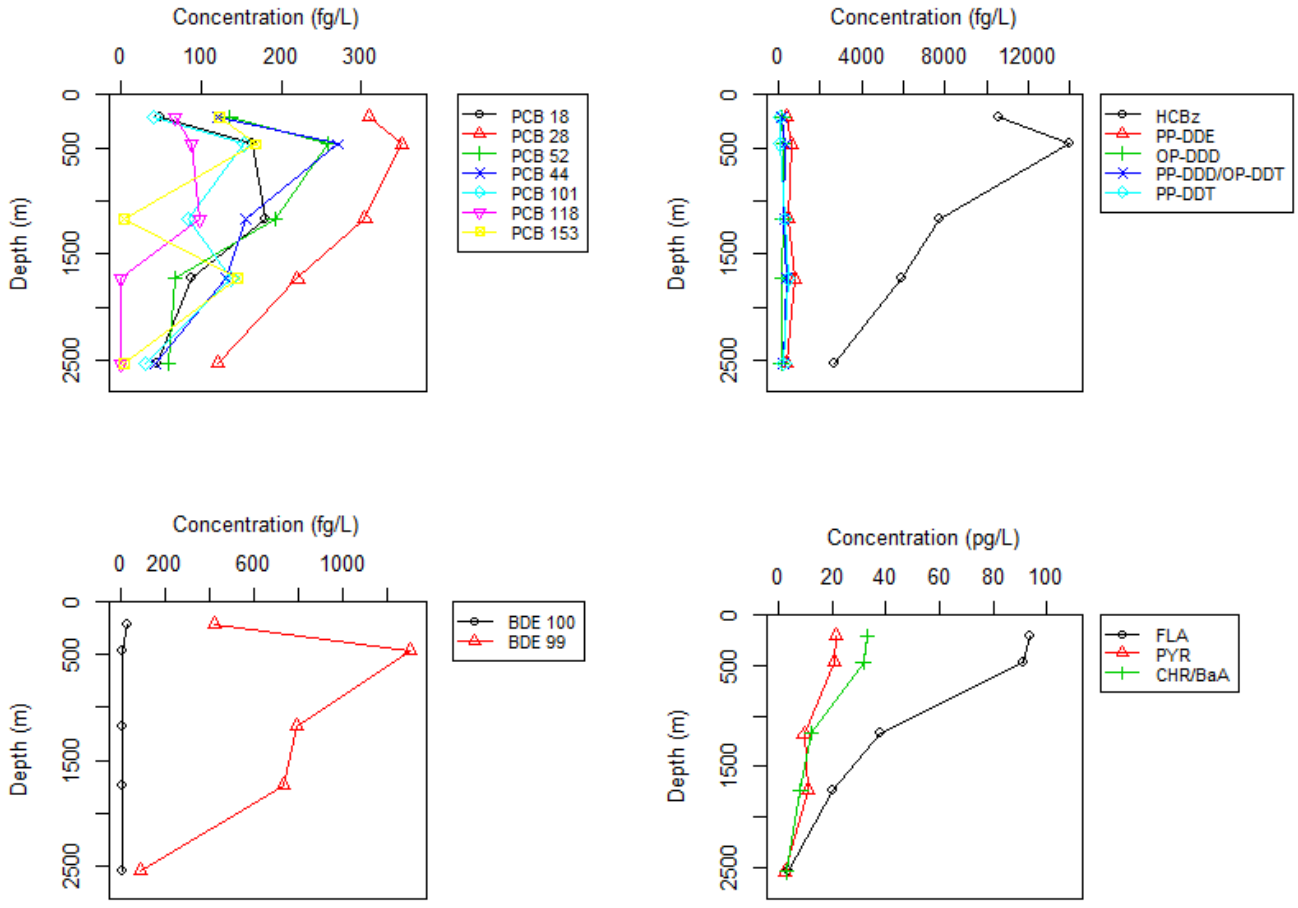

Figure 1.3 Depth profiles of POPs (PCBs, OCPs, PBDEs and PAHs) in the North Atlantic.

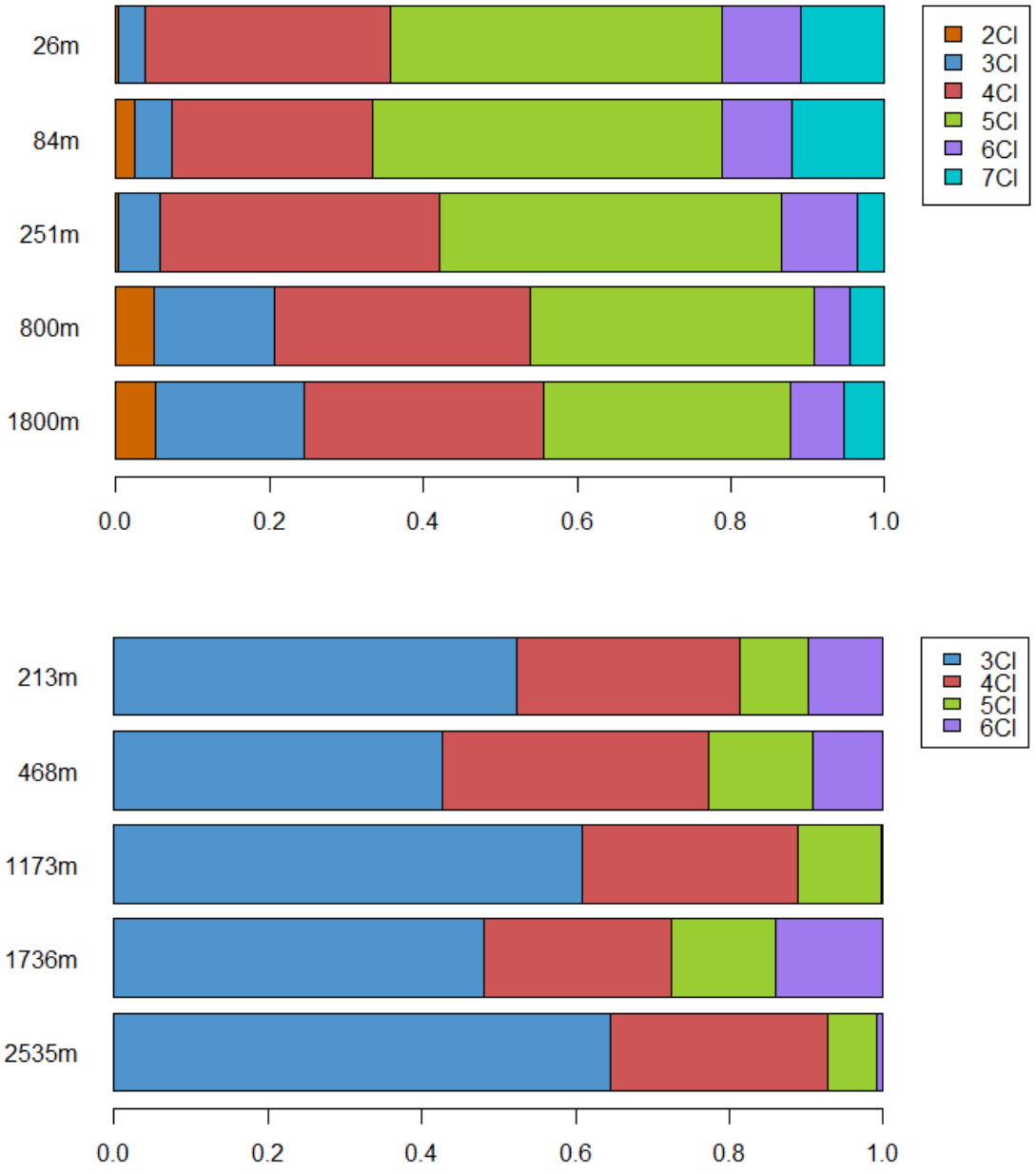

Figure 1.4 Composition of PCBs with different chlorinated degrees in the tropical Atlantic (top) and North Atlantic (bottom).

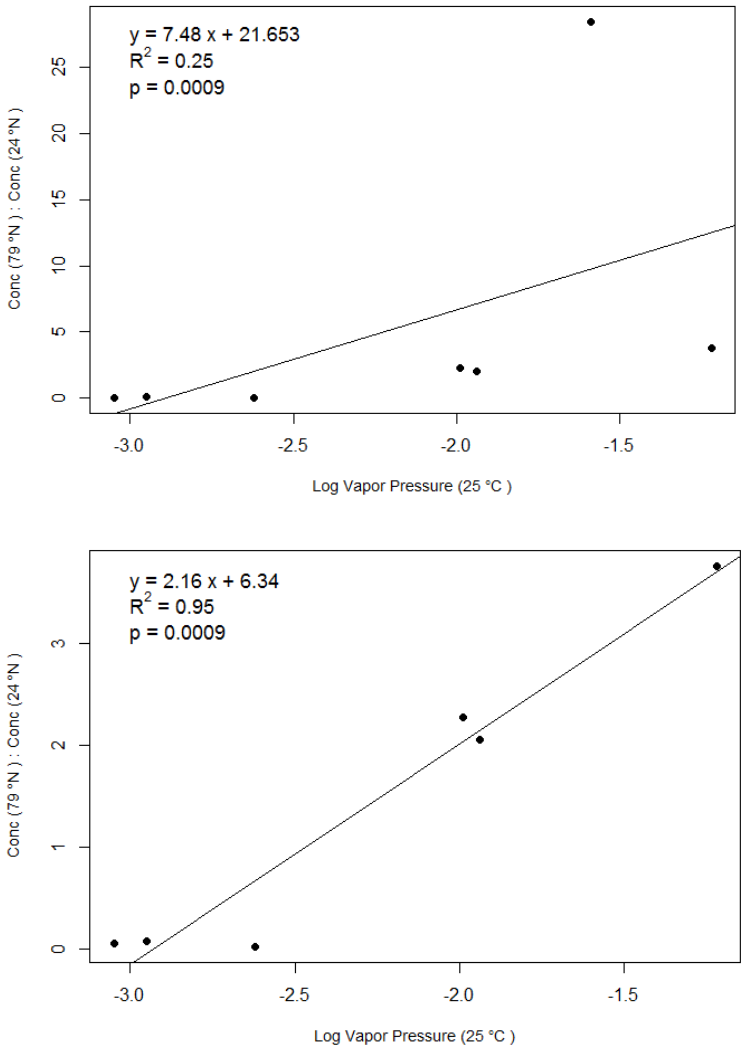

Figure 1.5 Ratio of the concentration at 79˚N and 24˚N for PCBs detected at the depth nearest to the surface at both sites, as a function of Log Vapor Pressure (Pa) at 25˚C (see Table S1). (Top: all PCBs detected at both sites; Bottom: PCB-28 removed as an outlier)

POPs concentration and air-seawater exchange comparison between the Pacific cruises

Manuscript in preparation for submission to *Environmental Science and Technology Letters*

Caoxin Sun[1], Erik Zettlerl[2] and Rainer Lohmann[1,*]

[1]Graduate School of Oceanography, University of Rhode Island, South Ferry Road, Narragansett, 02882 Rhode Island, United States

[2] Sea Education Associations, Woods Hole, 02543 Massachusetts, United Sates

ABSTRACT

Few studies measured the concentrations of POPs simultaneously in the atmosphere and surface seawater in the open Pacific Ocean. This study collected air and water samples using passive polyethylene across the Pacific Ocean in 2010 and 2012. Samples were analyzed for PCBs, OCPs, BDEs and PAHs. PCB-8 was detected at the highest concentration with gas-phase concentrations of 14 pg m^{-3} and dissolved concentration of 5.5 pg L^{-1} in the northern cruise in 2010. The other PCBs were all detected at around 1 pg m^{-3} in the air and 0.1 pg L^{-1} in the water. HCB dominated in the gas phase (~300 pg m^{-3}), while α -HCH dominated in the dissolved phase (~100 pg L^{-1}). Large variations of BDEs and PAHs concentrations in either phase were found and were higher than most reported values.

Close to equilibrium state of PCBs and OCPs were found in the oligotrophic Pacific. Absolute air-water exchange fluxes were <0.4 ng m^{-2} day^{-1} for PCBs and <4.5 ng m^{-2} day^{-1} for OCPs. Net air-water exchange gradients strongly favored gas-phase deposition of PBDEs into the water, while mixed gradients were found for PAHs.

INTRODUCTION

Very few studies have been made regarding POPs concentrations in the Pacific Ocean. Iwata et al. (1993) reported the first simultaneous measurement of air and water organochlorines across the global ocean. Results suggested various distribution patterns for different compounds (Iwata et al., 1993). Recently, Zhang & Lohmann (2010). reported the distribution of PCB and HCB in the Pacific Ocean; Gonzalez-Gaya et al. (2014) studied the global oceanic distribution of perfluorinated alkyl substances (PFASs) Simultaneous measurements of air and water samples allows the study of air-seawater exchange, which is critical to filling the gap of POPs global fate and behavior. Air-seawater exchange determines the distribution of POPs between two important compartments: atmosphere and surface open ocean. The concentration of POPs on the surface ocean further influences the efficiency of POPs removal into the deep ocean (Jones et al., 2004), which is a final sink for these POPs (Gioia et al., 2008b). Primary emissions of POPs to atmosphere have changed over the decades; ambient concentration declined as a result of reductions in primary emissions (Jones et al., 2004). Surface ocean received relatively high depositional input in the past. In the 1989/1990, a first global study covering the world's oceans reported PCBs and other POPs influx to the ocean (Lohmann et al., 2012b). Studies in Great Lakes and Baltic Sea suggest that water became the secondary source of PCBs to the atmosphere (Jones et al., 2004). It remains a question of the direction of air-seawater exchange in the open ocean. Most recent cruises studying air-water exchange of POPs were focused on the Atlantic Ocean. Close air-water equilibrium of PCBs was suggested for most of the Atlantic North-South transect with only a few regional deposition dominating over volatilization (Gioia et al., 2008b).

To the contrast, net volatilization of PCBs were suggested across an East-West transect near the tropical Atlantic (Lohmann et al., 2012b). From the same cruise, HCB were suggested to be near equilibrium while DDTs were indicated to be depositing into the ocean (Lohmann et al., 2012b). Net deposition of BDEs into the surface waters were implied in the tropical (Lohmann et al., 2013a) and southern Atlantic Ocean (Xie et al., 2011). PAHs were found to be undergoing net deposition across the tropical Atlantic Ocean, with conditions closer to equilibrium off the U.S. East Coast (Lohmann et al., 2013b). The only air-seawater exchange study in the Pacific so far reported volatilization of PCBs and near air-water equilibrium for HCB (Zhang & Lohmann, 2010).

This study collected air and water samples using polyethylene passive samplers with the help of Sea Education Association (SEA). Cruises were carried out onboard the SEA's sailing research vessel, SSV *Robert C. Seamans.*, as it sailed in 2010 and 2012, along an east-west transect in the Pacific Ocean. Polyethylene passive samplers measure the dissolved phase of POPs in air and water, simplifying the process of calculating air-water exchange gradient. The aims of this study were to (i) obtain dissolved phase and atmospheric concentration of POPs in the Pacific Ocean; (ii) discuss PE based net air-water exchange of POPs in the open ocean; (iii) compare results from different years/ latitudes.

METHODS

Sampling

PE Sheet Samplers Preparation and sample deployment

Polyethylene samplers (50 μm) preparations were discussed elsewhere (Chapter 1).

The PE air samplers were exposed in inverted stainless steel bowls. The water PE samplers were fixed in a steel pipe connected to the flowing seawater inside the ship's laboratory. Several PEs were deployed inside the ship at several locations including the science lab, galley and engine room.

There were two cruises altogether and both were conducted by the SEA research vessel in the Pacific. One Pacific cruise was conducted in 2010, it started from Hawaii Islands in early July 2010 and headed all the way east towards San Francisco Bay ending in late July 2010. The other Pacific cruise was conducted two years later, from early November 2012 (San Diego) and ending in early November 2012(Hawaii Islands). All the air and water samples collected were marked on Figure 2.1. The numbers on the figure represented the order of samples taken. For each number, there were one air and one water sample collected. In addition, in order to check the background contamination from the ship, PEs were deployed in the lab, engine room and galleys on the ship. All the detailed sampling information are given in Table S17.

Sample Analysis

Sample extraction and instrumental analysis were discussed elsewhere (Chapter 1).

Quality assurance/Quality control

QA/QC details were discussed elsewhere (Chapter 1).

Statistics of comparison between the cruises

Mann–Whitney *U* test were used for comparing the concentrations and fluxes of POPs between the cruises. The null hypothesis is that there is no difference of the distribution of POPs between the two cruises. A significant level of 0.05 was chosen.

For concentration comparison, one representative compound from each group (PCB, OCP, BDE, PAHs) was chosen. They were: PCB-11, HCB, BDE-47 and chrysene/benzo(a)anthracene. They were selected since they were the highest concentration among those detected at both cruises.

Air-Water Exchange Gradient and Flux Calculation

The gradient of air-water exchange is the ratio of the concentration of POPs in the PE at equilibrium with the air (C_{eqA}, ng/g) to the concentration at equilibrium with the water (C_{eqW}, ng/g):

$$\text{Gradient} = \frac{C_{iw} \times K_{iaw}}{C_{ia}} - 1$$

Air water exchange flux was calculated by Whitman two-film model:

$$F = k_{i\ a/w} \left(C_{iw} - \frac{C_{ia}}{K_{iaw}}\right)$$

Where k_{ol} is the mass transfer coefficient ($cm \cdot s^{-1}$), which can be calculated by:

$$\frac{1}{k_{i\ a/w}} = \frac{1}{k_{iw}} + \frac{1}{k_{ia} \cdot K_{iaw}}$$

$$k_{ia} = (0.2\, u_{10} + 0.3)\,.\left[\frac{D_{ia}}{D_{H_2O\,a}}\right]^{0.67};$$

$$k_{iw} = \left(\frac{Sc_{iw}}{600}\right)^{-0.5}\,.\left[\frac{D_{iw}}{D_{CO_2\,w}}\right]^{0.5}$$

$$u_{10} = u_z\,.\left(\frac{10.4}{\ln(z)+8.1}\right)$$

where u_{10} and u_z are the wind speeds measured 10 m and z m above the water surface, D_a and D_w are diffusivity coefficient in air and water respectively which can be calculated as :

$$D_{ia} = 10^{-3}\,\frac{T^{1.75}\left[1/M_{air} + 1/M_i\right]^{0.5}}{p\left[\overline{V}_{air}^{1/3} + \overline{V}_i^{1/3}\right]^2}\ (cm^2 s^{-1});\qquad D_{iw} = \left[\frac{13.26 \times 10^{-5}}{\mu^{1.14} \times \overline{V}_i^{0.589}}\right]$$

where T is the absolute temperature (K), M_{air} is the average molar mass of air (28.97 g mol^{-1}), M_i is the chemical's molar mass (g mol^{-1}), p is the gas phase pressure (atm), Vair is the average molar volume of the gases in air (20.1 cm^3 mol^{-1}), Vi is the chemical's molar volume (cm^3 mol^{-1}), μ is the water viscosity at T (10^{-2} g cm^{-1} s^{-1}).

RESULTS AND DISCUSSION

Concentration comparison with literature

Pacific (2010)

Average concentrations from the present study were based on 4 samples from each cruise (the coastal sample was removed). All POPs detected were plotted in Figure 2.2. PCB-8, 11, 28, 153, 206 were the detected congeners in the Pacific 2010 cruise, with PCB-8

detected at the highest average concentration of 14 pg m^{-3} and the others ranging between 0.8~3.5 pg m^{-3}. Similarly, for the dissolved phase, averaged PCB-8 was dominant at 5.5 pg L^{-1} and the other congeners were 0.1-0.9 pg L^{-1}.

HCB was detected at 340 pg m^{-3} in the air and 12 pg L^{-1} in the water. HCHs were more dominant in the water than in the air, and α-HCH was detected at higher concentration than ϒ-HCH in both air and water. In the atmosphere, the concentration of detected ∑HCHs (α-HCH, ϒ-HCH) were ~30 times smaller than found by Iwata et al. (1993), while the ∑CHLs (*t*-chlor, *c*-chlor, *t*-nona) were only 10 times smaller. However, the concentration ranges of α-HCH and ϒ-HCH (14-35 and 1.4-4 pg m^{-3}) were consistent with more recent studies: (6.5-19 and 1-4.6 pg m^{-3}) by Ding et al. (2007) and (26-56 and 10-36 pg m^{-3}) by Wu et al. (2010). HCHs were dominant by α-HCH (90%) and followed by ϒ-HCH (10%); this α/ ϒ ratio is higher than detected in Northeast Asia where α-HCH (71%) and ϒ-HCH (23%) were found (Baek et al., 2013) . The reason is that long range atmospheric transport (LRAT) causes an increase in α/ϒ-HCH ratio by either direct partitioning into seawater or through washout by precipitation (Ding et al., 2007). In the dissolved phase, a similar ratio of ∑HCHs to the ∑CHLs was observed - 110 from this study compared to the ratio of 120 (Iwata et al., 1993), although the absolute concentration from this study are 10 times smaller than detected 15 years ago.

BDE-47 and 99 were the two dominant congeners in the air (21 pg m^{-3} and 15 pg m^{-3} respectively). Concentrations were 40 times lower during a cruise from east Asia to the Arctic (Möller et al., 2011). Larger concentration of BDEs was also found of dissolved phase from this study.

Biphenyl, acenaphthene, fluorene, fluoranthene, pyrene, retene, benzo(a)anthracene, chrysene, benzo(b/k)fluoranthene were the detected PAHs, which were also detected during a cruise from east Asia to the Arctic except for biphenyl and retene (Ma et al., 2013). Much higher concentrations in the atmosphere were found from this study; acenaphthene on average of four samples were 50 times higher than reported North Pacific maximum from (Ma et al., 2013), and the other congeners were around 10 times higher from this study (Ma et al., 2013). However, there were great variations between the four air samples in this study as well. A-3 was collected in the open North Pacific ocean near Seattle and the concentration of ∑PAHs (acenaphthene, fluorene, fluoranthene, pyrene, benzo(a)anthracene, chrysene, benzo(b/k)fluoranthene) (240 pg m^{-3}) were very close to the North Pacific average of ∑PAHs of the same compounds reported (181 pg m^{-3}) by (Ma et al., 2013). Similarly, large variations between samples also occurred for water samples that much smaller concentrations were detected from W-4 (178 pg L^{-1}) than the other water samples.

Pacific (2012)

All POPs detected were plotted in Figure 2.3. PCB-101, 118, 153, 169 and 189 were detected in the Pacific Ocean in 2012, with atmospheric concentrations averaging 0.1-0.6 pg m^{-3} and dissolved concentration between 0.6-1.3 pg L^{-1}. These results are comparable to concentrations reported as 1.6-3.2 pg m^{-3} and 0.7-2.0 pg L^{-1} for the mean of PCB-101, 118 and 153 in the Northern Pacific (Zhang & Lohmann, 2010). Results from both studies were much lower than reported by Iwata et al. (1993), in which 130 pg m^{-3}

(atmosphere) and 24 pg L^{-1} (seawater) were detected for ∑PCB in the Northern Pacific (Iwata et al., 1993).

HCB, α-HCH and ϒ-HCH were detected as OCPs. HCBs dominated in the air (220 pg m^{-3}) while HCHs dominated in the dissolved phase (~140 pg L^{-1}). HCB from this study (220 pg m^{-3} and 9 pg L^{-1}) were much higher than (61 pg m^{-3} and 0.9 pg L^{-1}) (Zhang & Lohmann, 2010); while close to the upper range for atmosphere background in Japan (137 pg m^{-3}) (Murayama et al., 2003) and seawater average for the northern hemisphere (12 pg L^{-1}) (Barber et al., 2005). α-HCH and ϒ-HCH were detected at close concentrations, which were ~10 pg m^{-3} and ~140 pg L^{-1} in the air and seawater, respectively.

BDE-28, 47 and 99 were detected, with 47 and 99 dominant at ~5 pg m^{-3} in the atmosphere and BDE-47 dominant at 11 pg L^{-1} in the seawater. Concentrations were higher than the gas phase of BDEs near east Asia: BDE-47 and 99 detected at < 0.5 pg m^{-3} (Möller et al., 2011). W-1 and A-5 were not included in the calculation, because their abnormal extreme large concentrations were potentially affected by inland or ship contamination and were not representative of remote ocean concentrations.

Phenanthrene, fluoranthene, pyrene, and chrysene /benzo(a)anthracene were the detected PAHs. Phenanthrene showed the largest concentration in air (140 pg m^{-3}) and seawater (500 pg L^{-1}). The other PAHs were at ~ 10 pg m^{-3} and ~ 100 pg L^{-1}.

The averages of PCBs and OCPs concentrations from the Pacific cruises were close to literature data, while BDEs and PAHs data were much greater. However, there were large variation between different samplers regarding BDEs and PAHs. One or two samplers yielded BDE and PAH data comparable to reported concentrations. Therefore, it is

unlikely that contamination influenced all the samplers during the Pacific cruises. Yet overall, the comparison of results suggests that some of the data reported for PAHs and PBDEs was not characteristic of open ocean values, but was either influenced by continental air or contaminated during sampling.

Concentration comparison between cruises

Table 2.1 summarized the results for POPs concentration comparison between the two cruises. As to the comparison of detected single compound and sum of each group, there were more significant differences between the two cruises in the ocean than in the atmosphere. This indicated that POPs in the atmosphere are more homogeneously distributed.

For PCBs, although the northern cruise suggested higher atmospheric ∑PCB values, no significant difference in dissolved phase ∑PCB was seen and a higher PCB-153 concentration was detected from the southern cruise.

For OCPs, there was only significant difference of ∑OCP in the dissolved phase which was very likely to be caused by HCHs. $[\alpha\text{-HCH}]_{diss}$ and $[\alpha\text{-HCH}]_{diss}$ were revealed to be positively correlated to latitude (Xie et al., 2011); while this was not seen in this study. In general, there were larger variations between samples in the northern cruise, indicating more even POPs distribution along the San Diego-Hawaii transect than along the San Francisco Bay-Hawaii transect.

Air-water exchange gradients

Significant departure from equilibrium was considered as gradient outside of 0.137-3.91 (Ruge, 2013). Any gradients values larger than 3.91 was considered as evaporation; any values smaller than 0.137 were considered as deposition.

Air-water exchange gradients were plotted in Figure 2.4. PCBs and OCPs displayed equilibrium/evaporation for both cruises; BDEs and larger PAHs favored deposition for Pacific 2010 cruise while most BDEs and PAHs favored evaporation for Pacific 2012.

A detailed air-water exchange gradients values for each single sample were displayed in Table S17. One thing to note is that A/W-1 and A/W-5 from Table S17 were not used for plotting Figure 2.4 or Figure 2.5 due to the extreme values observed for BDEs.

For cruise Pacific 2010, more deposition was indicated for A/W-4 than the other three samples. A/W-4 collection included a three-day anchor in San Francisco Bay. As upwelling occurs near coastal California, productivity is high thus taken away $[PCB]_{diss.}$ Also, the sampling location of A/W-4 was close to land emission and could thus be affected by land emissions (Lohmann et al., 2012b).

To the contrast, sampling areas for the other samples were mostly subtropical ocean gyres where productivity is low. There was very limited particle binding process to remove $[PCB]_{diss}$ resulting in large seawater dissolved concentrations. Combined with the reduction in ambient concentration in response to ceased PCB production, volatilization was favored in the open ocean as reported in the Pacific (Zhang & Lohmann, 2010) and in the tropical Atlantic by Lohmann et al. (2012b).

Similarly, OCPs favored equilibrium/evaporation for most samples, with a few exceptions of deposition for *cis*- chlordane and *trans*-nonachlor (Table S17). HCBs were at equilibrium for all samples collected from two cruises, in agreement with findings

from (Zhang & Lohmann, 2010). HCHs suggested evaporation/equilibrium in this study. Results for ϒ-HCHs from other studies are a mix. Some were dominated by net deposition such as in the North Atlantic/Arctic region (Harner et al., 1999; Jantunen et al., 2008; Lohmann et al., 2009) ; one study suggested net volatilization in the Pacific/Arctic region (Ding et al., 2007).

BDEs strongly favored deposition in most Pacific 2010 samples (Figure 2.4 and Table S17), in accordance with the other studies (Lohmann et al., 2013a). Unlike PCBs that the remote oligotrophic ocean became secondary source (Lohmann et al., 2012b; Zhang & Lohmann, 2010), most BDEs were only banned in the past decade. The atmospheric concentrations of BDEs were still high and air-seawater equilibrium has not been reached. However, some evaporations were seen for Pacific 2012 samples (Figure 2.4 and Table S17). Highly BDE polluted ocean water could have possibly contributed to this phenomenon. Similar discussion can be applied to PAHs gradients.

Air-water exchange fluxes comparison with literature

Fluxes calculated using a micrometeorological approach was compared with results using the Whitman two-film model in (Wong, 2010). The relative standard deviation (RSD) were estimated as 83-277% for the micrometeorological calculated flux (F_M) and 127-288% for the two-film model calculated flux (F_{TF}). For all events except for event #14, mean F_M was 0.44 ± 0.2 ng m^{-2} h^{-1} and mean F_{TF} was 0.29 ± 0.15 ng m^{-2} h^{-1}. The good agreement of RSD and mean fluxes calculated from the two methods validated the usage of either method. In the present study, a similar uncertainty 51% (0.15/0.29) for fluxes was adopted as from (Wong, 2010).

Averaged fluxes over all samples from each cruise were plotted in Figure 2.5. The overall air-water exchange fluxes of PCBs for the two cruises ranged from -0.04 ± 0.02 to 0.34 ± 0.17 ng m^{-2} day^{-1}, smaller range than fluxes from another study (0.5 - 30 ng m^{-2} day^{-1}) (Zhang & Lohmann, 2010). Averaged fluxes for HCB was -0.35 ± 0.18 and 0.26 ± 0.13 ng m^{-2} day^{-1} for 2010 and 2012, respectively. For HCHs, their averaged fluxes were -1.3 ± 0.66 to 4.5 ± 3.0 ng m^{-2} day^{-1} for α-HCH and -0.3 ± 0.15 to 1.6 ± 0.8 ng m^{-2} day^{-1} for ϒ-HCH, close to Xie et al. (2011) where mean deposition of 3.8 ng m^{-2} day^{-1} (α-HCH) and 2 ng m^{-2} day^{-1} (ϒ-HCH) were found in a north-south transect in the Atlantic ocean (Xie et al., 2011). The results were also comparable to (α-HCH: -6.8 to 7.7 ng m^{-2} day^{-1}) and (ϒ-HCH: -12 to -1.3 ng m^{-2} day^{-1}) (Zhang et al., 2012). No significant difference in air-water exchange fluxes between the two years were found (Table 2.1).

The fluxes for BDEs and PAHs in this study could be biased due to the high concentrations detected in the air and water, so that the discussion was moved to Supporting Information.

SUMMARY

This study adds to the current database of POPs distribution in the East Pacific Ocean. Several samples from this study revealed similar background concentrations of PCBs and OCPs as detected in the West Pacific. Comparison between cruises indicated that atmosphere was better mixed than surface seawater. Air-water exchange gradients in the Eastern Pacific suggested net volatilization/equilibrium in the oligotrophic regions for most PCBs and HCB, in line with findings from previous studies.

TABLES AND FIGURES

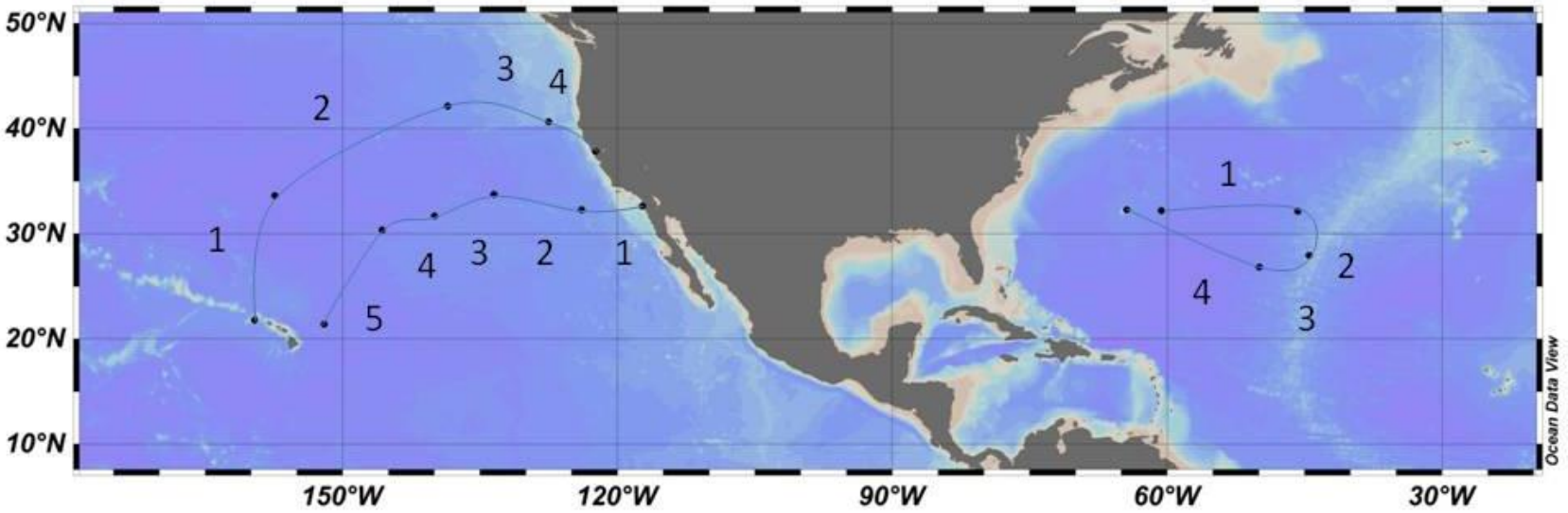

Figure 2.1 Sampling locations during the SEA cruise. (Atlantic cruise in the map is discussed in details in the Supporting Information.)

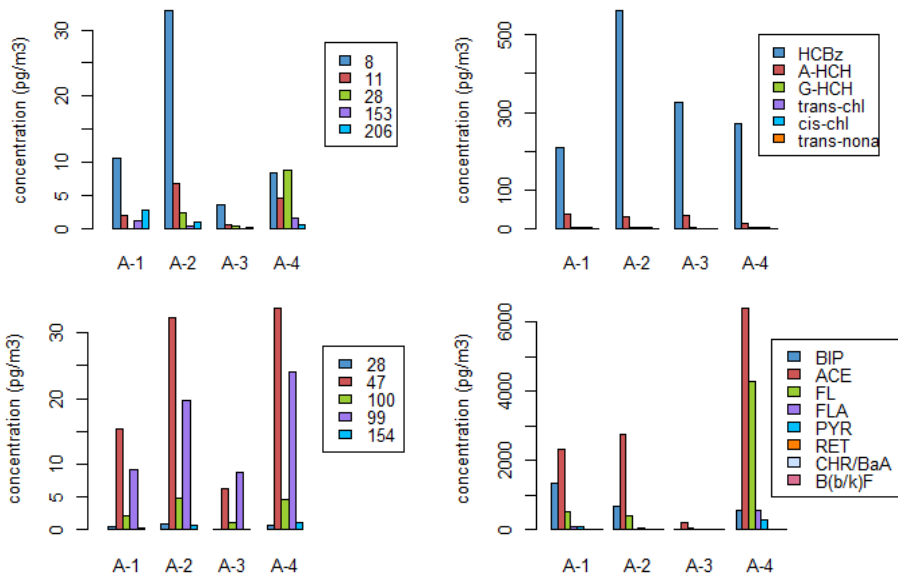

(top)

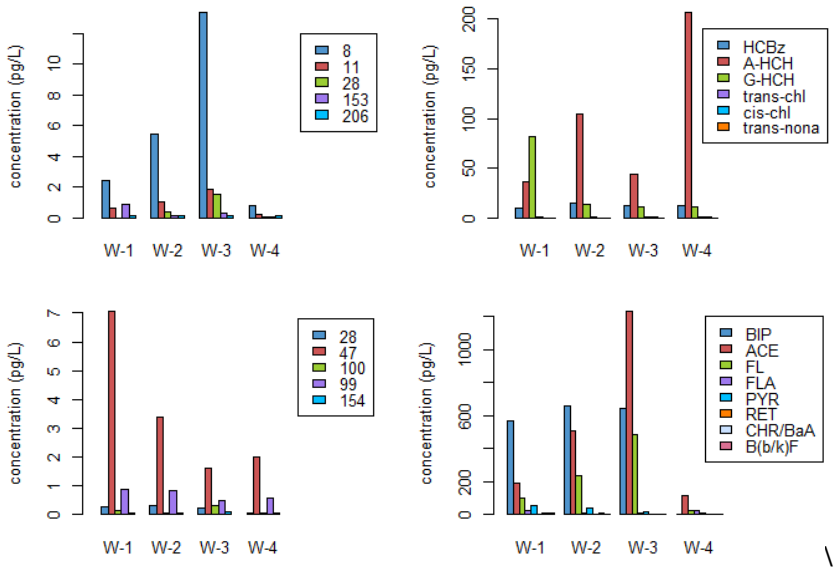

(bottom)

Figure 2.2 Atmospheric (top 4 panels) and dissolved (bottom 4 panels) of PCBs, OCPs, BDEs and PAHs in the Pacific 2010.

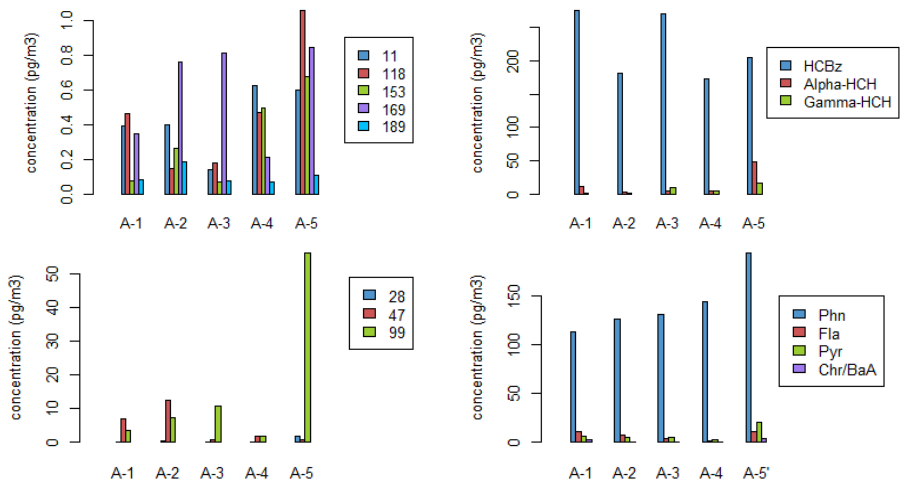

(top)

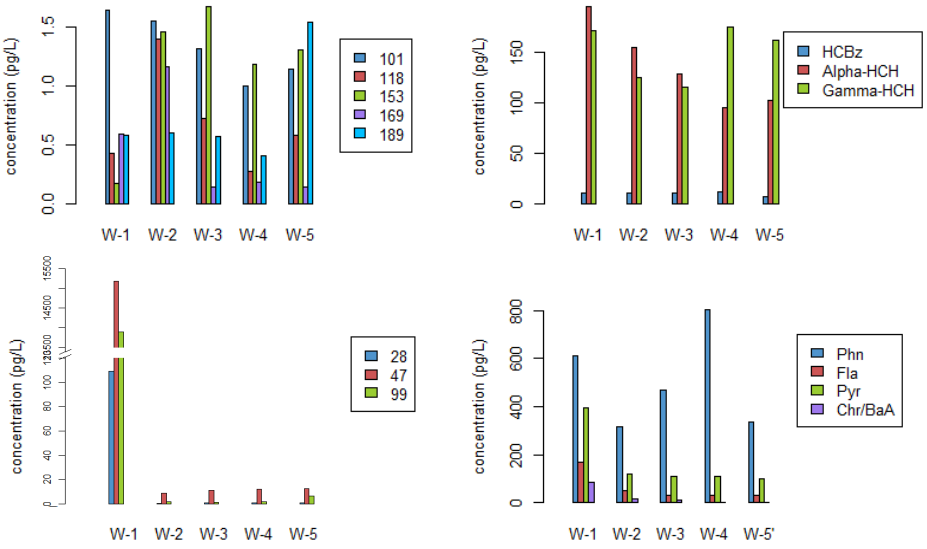

(bottom)

Figure 2.3 Atmospheric (top 4 panels) and dissolved (bottom 4 panels) concentration of PCBs, OCPs, BDEs and PAHs in the Pacific 2012.

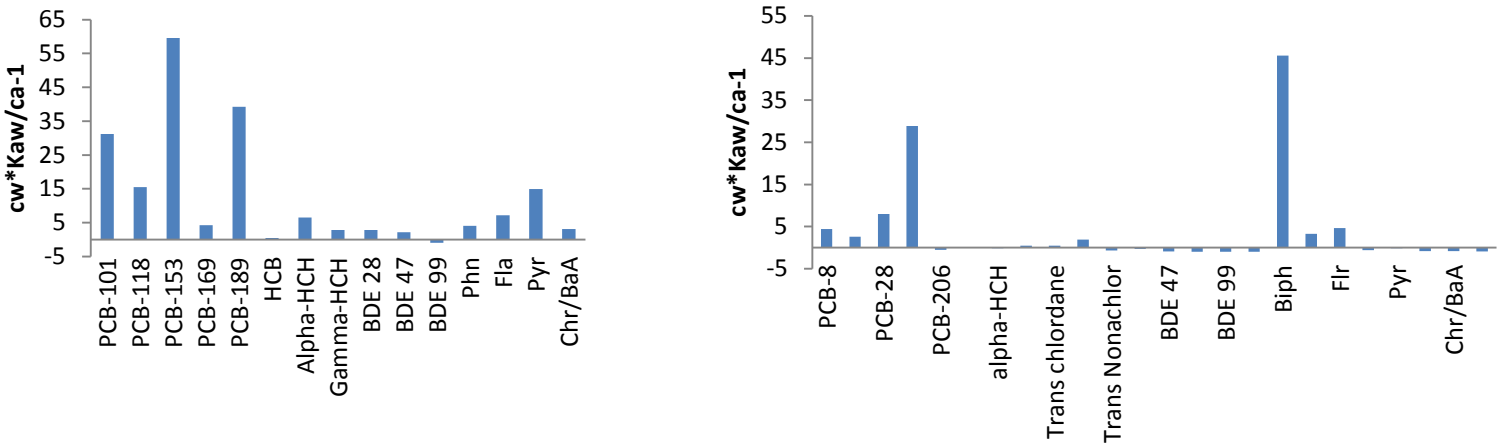

Figure 2.4 Averaged air-water exchange gradients of PCBs, OCPs, BDEs and PAHs from the two cruises. Left: 2012 Cruise; Right: 2010 Cruise

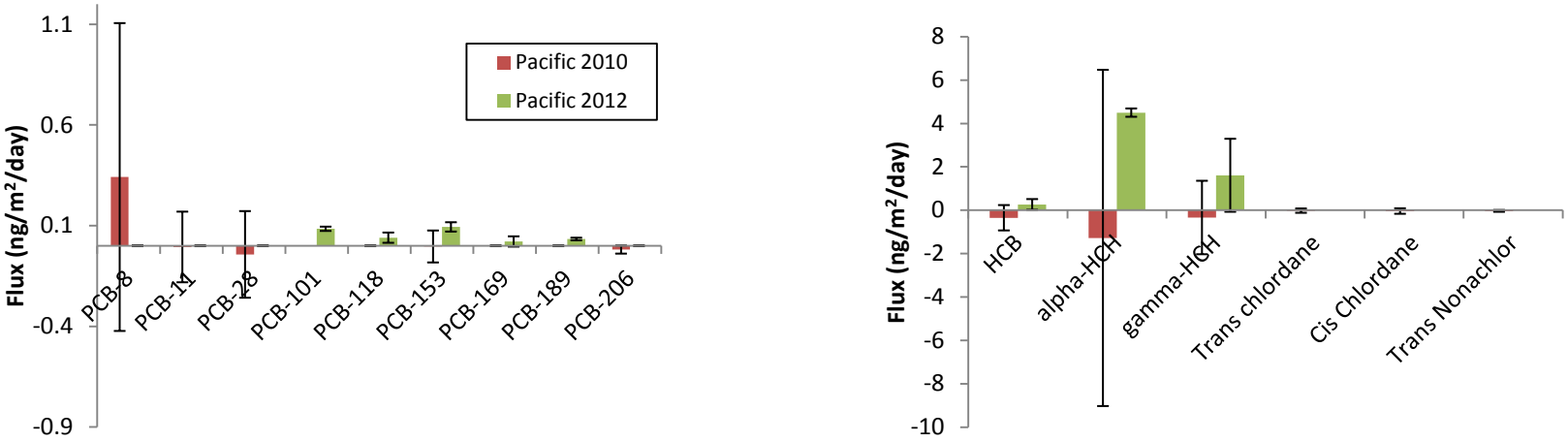

Figure 2.5 Averaged air-water exchange fluxes of PCBs and OCPs from the two cruises.

Error bars represent standards deviation between samples from each cruise.

Table 2.1 Comparison of air and water POPs concentrations and fluxes in the Pacific 2010 and 2012.

	mean		standard deviation		p-value
	Pacific 2010 (n=4)	Pacific 2012 (n=4)	Pacific 2010 (n=4)	Pacific 2012 (n=4)	
air samples					
PCB-153	0.80	0.23	0.76	0.20	0.49
hexachlorobenzene	341.52	224.76	155.01	55.58	0.34
BDE-47	21.99	5.43	13.44	5.44	0.11
benzo(b/k)fluoranthene	12.20	1.25	8.53	1.16	0.06
∑PCB	22.1	1.6	16.2	0.3	0.03
∑OCP	374.7	234.3	156.3	59.2	0.11
∑BDE	41.6	11.5	23.6	6.9	0.06
∑PAH	5149.5	139.5	4985.4	6.0	0.03
water samples					
PCB-153	0.33	1.40	0.38	0.21	0.03
hexachlorobenzene	12.22	9.61	2.43	1.93	0.20
BDE-47	3.52	11.13	2.48	1.72	0.03
benzo(b/k)fluoranthene	5.98	7.08	2.02	6.78	1.00
∑PCB	7.4	4.6	6.9	1.3	0.89
∑OCP	140.3	274.2	66.7	15.7	0.03
∑BDE	4.6	14.8	2.7	3.8	0.03
∑PAH	1249.1	631.9	934.5	219.4	0.34
fluxes					
	Pacific 2010 (n=4)	Pacific 2012 (n=3)	Pacific 2010 (n=4)	Pacific 2012 (n=3)	
PCB	0.27	0.27	1.18	0.01	0.40
OCP	-2.08	6.37	6.64	1.79	0.11

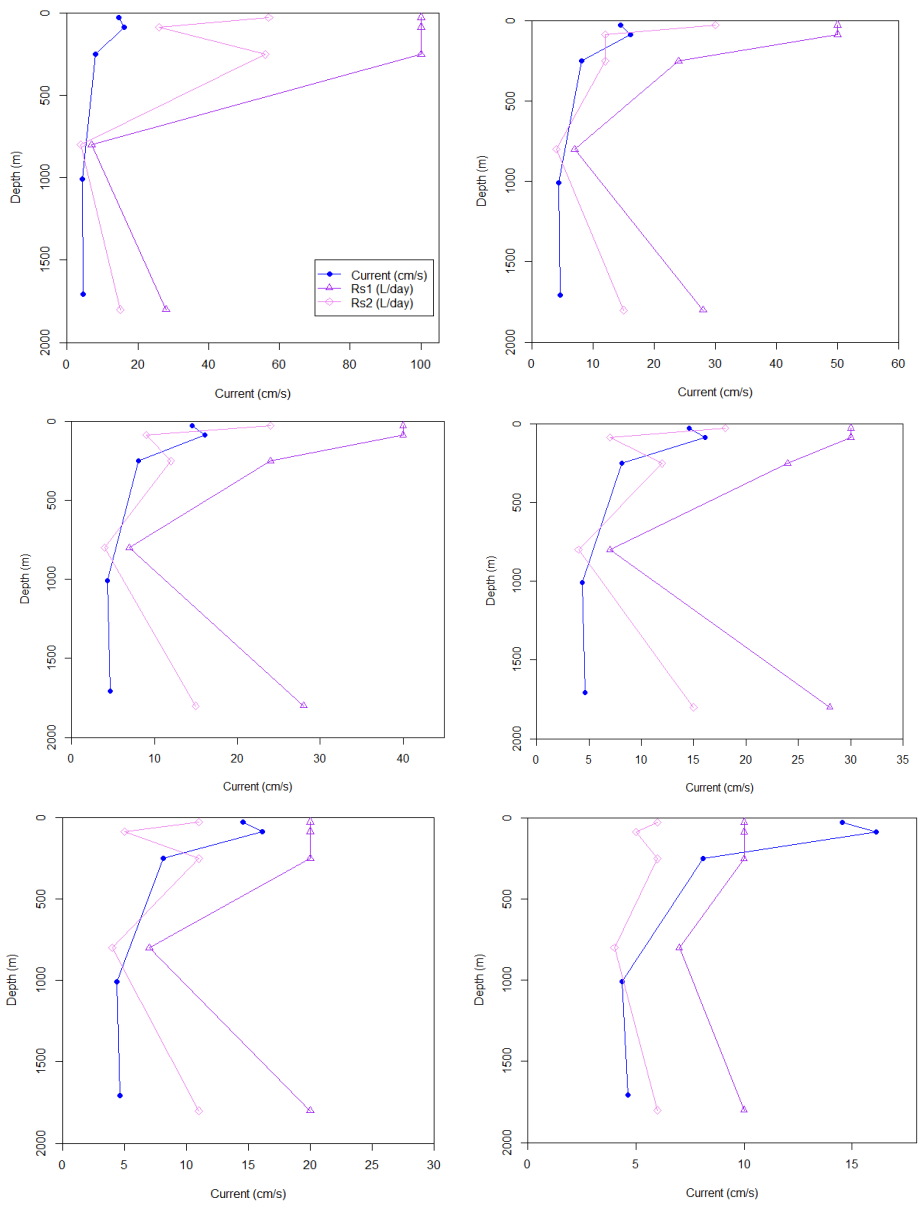

Figure S1. Estimated sampling rate under different range assumptions and comparison with current speed measurement (Tropical Atlantic).
Range of sampling rate assumptions: (Top left) 1~100 L/day;
(Top right) 1~50 L/day;
(Middle left) 1~40 L/day;
(Middle right) 1~30 L/day;
(Bottom left) 1~20 L/day;
(Bottom right) 1~15 L/day.
Line colors: (blue) current speed in cm/s;
(purple) Rs in L/day of 800 μm PEs;
(pink) Rs in L/day of 1600&50 μm PEs.

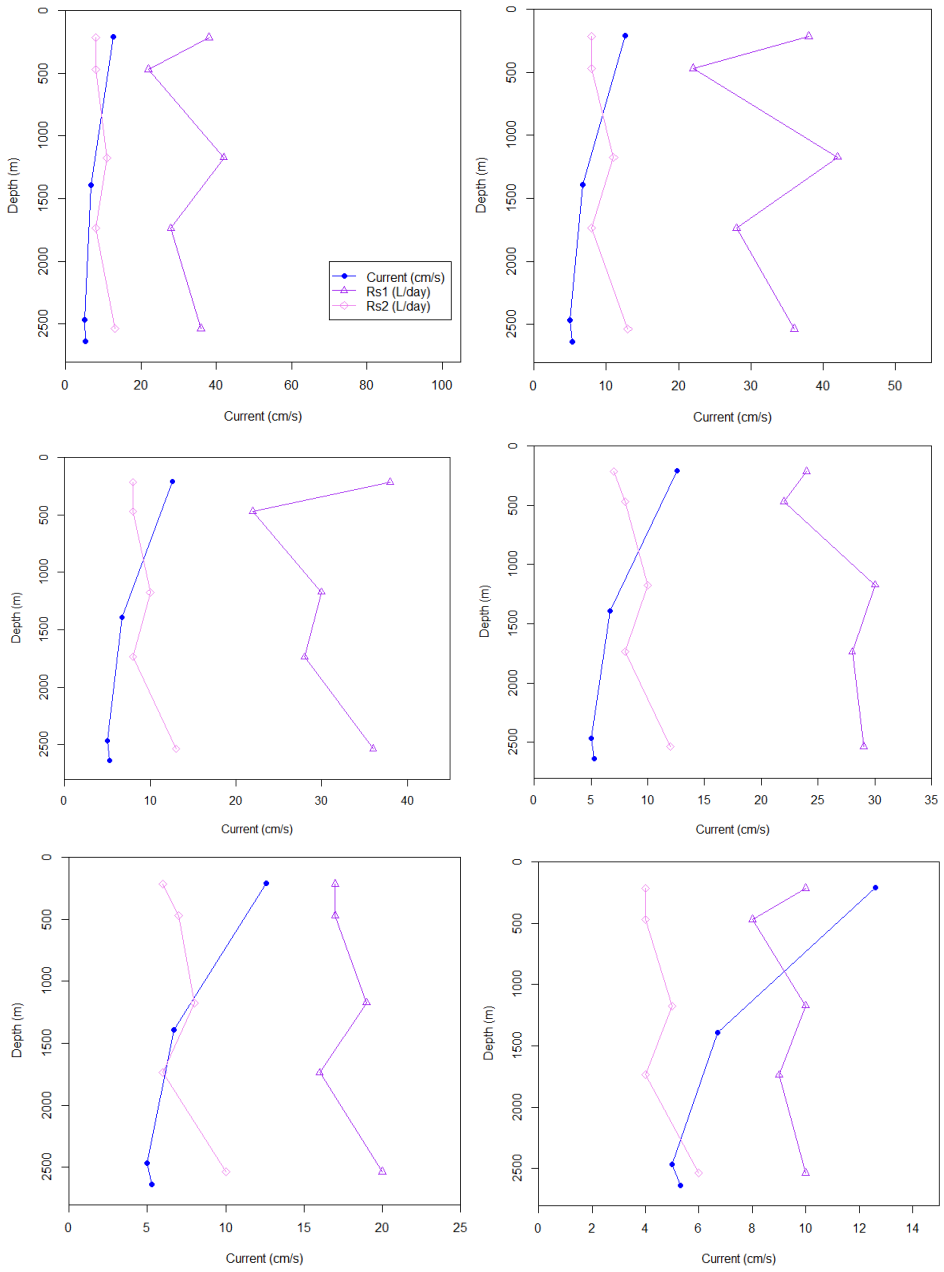

Figure S2. Estimated sampling rate under different range assumptions and comparison with current speed measurement (North Atlantic).
Range of sampling rate assumptions: (Top left) 1~100 L/day;
(Top right) 1~50 L/day;
(Middle left) 1~40 L/day;
(Middle right) 1~30 L/day;
(Bottom left) 1~20 L/day;
(Bottom right) 1~15 L/day.
Line colors: (blue) current speed in cm/s;
(purple) Rs in L/day of 800 μm PEs;
(pink) Rs in L/day of 1600 μm PEs.

Table S1. Dissipation of PRCs in Tropical Atlantic moorings.

	84 m	800 m
d_8-naphthalene	100%	100%
d_{10}-pyrene	100%	98%
d_{12}-benzo(a)pyrene	84%	14%
PBB 9	100%	100%
PBB 52	95%	100%
PBB 103	0%	3%
OCN	0%	0%

Table S2. Physico-chemical constants (at 25 ˚C) used in this study.

PCBs	**log K_{PE-W} (L/kg)[a]**	**log K_{AW}[b]**	**ΔH_{VAP} (KJ/mol)[c]**	**log P_L (Pa)[b]**
PCB 8	4.5	-2.06	72	-0.86
PCB 11	4.93	-2.16	75	-1.21
PCB 18	4.9	-2.07	75	-1.22
PCB 28	5.4	-1.93	78	-1.59
PCB 44	5.5	-2.04	81	-1.99
PCB 52	5.7	-1.96	81	-1.94
PCB 66	6	-1.92	85	-2.53
PCB 101	6.3	-2.08	85	-2.67
PCB 118	6.4	-2.36	89	-3.05
PCB 153	6.8	-2.13	91	-3.26
PCB 105	6.4	-2.39	89	-3.05
PCB 138	7	-1.97	92	-3.27
PCB 187	7.1	-1.64	94	-3.78
PCB 128	6.6	-1.95	93	-3.51
PCB 180	7.1	-2.51	97	-3.88
PCB 169	7.39	-2.1	99	-4.21
PCB 189	7.72	-2.01	100	-4.35
PCB 206	8.16	-2.3	103	-4.95
OCPs[d]	**log K_{PE-W} (L/kg)**	**log K_{AW}**	**ΔH_{VAP} (KJ/mol)**	**log P_L (Pa)**
Hexachlorobenzene	5.2	-1.5	69	-1.03
α-hexachlorocyclohexane	2.8	-3.6	69	-0.59
γ-hexachlorocyclohexane	3	-4.1	71	-1.12
Trans- chlordane	5.2	-2.5	81	-2
Cis- chlordane	5.2	-2.7	80	-2.14
Trans- nonachlor	5.7	-3	83	-2.43
p,p'-DDE	5.5	-2.8	86	-2.47
o,p'-DDD	5.1	-3.7	98	-3.77
p,p'-DDD	5	-3.7	89	-2.92
o,p'-DDT	5.7	-3	89	-2.84
p,p'-DDT	5.8	-3.3	93	-3.32

a) from (Lohmann, 2012a) and greyed values from (Khairy & Lohmann, 2014)
b) final adjusted values from (Schenker, Macleod, Scheringer, & Hungerbühler, 2005). Greyed values for K_{aw} were calculated using equations from (Khairy & Lohmann, 2014) and using Henry's law constant from (Mackay et al., 2006); Greyed values for P_L were calculated using equations from (Khairy & Lohmann, 2014) using P_L from (Renee L. Falconer, 1994).
c) from (Komp & McLachlan, 1997) and greyed values from (Khairy & Lohmann, 2014)
d) from (Khairy & Lohmann, 2013)

Table S2. Cont'd. Physico-chemical constants (at 25 ˚C) used in this study.

BDEs	**log K_{PE-W} (L/kg)[a]**	**log K_{AW} [b]**	**ΔH_{VAP} (KJ/mol)[c]**	**log P_L (Pa)[b]**
BDE-15	5.1	-2.78	67.6	-2
BDE-28	5.7	-3.11	79.7	-2.8
BDE-47	6.3	-3.35	94.6	-3.67
BDE-99	6.9	-3.67	108	-4.44
BDE-100	6.9	-3.81	102	-4.43
BDE-154	7.4	-3.94	113	-5.04
BDE-153	7.4	-3.86	110	-5.05
BDE-183	7.98	-4.22	118	-5.38

PAHs	**log K_{PE-W} (L/kg)[d]**	**log K_{PE-A} (L/kg)[e]**	**ΔH_{VAP} (KJ/mol)[f]**	**log P_L (Pa)[f]**
Biphenyl	3.5	6.1	68	0.19
Acenaphthylene	3.5	5.9	67	0.3
Acenaphthene	3.6	6	68	0.19
Fluorene	3.9	6.4	74	-0.46
Phenanthrene	4.2	7	80	-1.1
Fluoranthene	4.9	8	91	-2.4
Pyrene	4.9	8.1	91	-2.4
Retene	5.7	9.4	106	-4.13
Benz[a]anthracene	5.6	9	104	-3.81
Chrysene	5.6	9.4	104	-3.81
Benzo[b]fluoranthene	6.2	10.3	115	-5.1
Benzo[k]fluoranthene	6.2	10.4	115	-5.1

a) from (Lohmann, 2012a)
b) final adjusted values of (Wania & Dugani, 2003). Grayed values were calculated using equations from (Khairy & Lohmann, 2014).
c) final adjusted values of (Tittlemier et al., 2002). Grayed values were calculated using equations from (Khairy & Lohmann, 2014).
d) from (Lohmann, 2012a)
e) from (Khairy & Lohmann, 2014)
f) ΔH_{VAP} values using regression line from (Rene P. Schwarzenbach, Philip M. Gschwend, 2002) and P_L values from (Y. G. Ma, Lei, Xiao, Wania, & Wang, 2010)

Table S3. Detection limit of PCBs for mooring samplers.

Compound	Average Field Blank Concentration(pg/g PE)	STDEV	Detection Limit (pg/g PE)	Detection[a] Limit (fg/L)	% Detection (Tropical Atlantic)	% Detection (North Atlantic)
PCB 8	17	1.4	4.1	130	90	0
PCB 11	41	11	33	387	10	0
PCB 18	16	0.67	2.0	25	60	80
PCB 28	27	0.13	0.40	1.6	100	90
PCB 44	11	7.0	21	67	90	50
PCB 52	31	10	30	62	90	40
PCB 66	5.8	4.7	14	17	50	20
PCB 81	12	2.5	7.6	7.2	0	0
PCB 77	19	20	61	58	0	0
PCB 101	24	2.6	7.7	6.4	100	60
PCB 118	6.6	0.027	0.08	0.06	100	40
PCB 123	4.8	0.11	0.34	0.23	0	0
PCB 114	6.5	0.24	0.73	0.52	0	0
PCB 105	10	1.4	4.3	3.3	90	0
PCB 126	15	2.5	7.5	4.8	0	0
PCB 153	2.2	0.68	2.1	1.3	100	50
PCB 138	9.2	8.7	26	16	100	20
PCB 128	11	11	34	24	40	0
PCB 167	16	16	48	28	0	0
PCB 156	6.3	4.3	13	7.5	0	0
PCB 157	11	13	40	24	0	0
PCB 169	20	20	61	35	0	0
PCB 187	12	10	31	19	100	0
PCB 180	39	5.4	16	10	90	0
PCB 170	19	22	65	38	0	0
PCB 189	32	21	62	34	0	0
PCB 195	22	8.7	26	15	0	0
PCB 206	33	2.3	6.8	3.8	0	10
PCB 209	2.3	0.60	1.8	1.0	0	10

a) Estimated typical ambient detection limit using deployment time 380 days, sampler mass 11.5 g, and water sampling rates (50 L/day)

Table S3. Cont'd. Detection limit of OCPs for mooring samplers.

Compound	Average Field Blank Concentration(pg/g PE)	STDEV	Detection Limit (pg/g PE)	Detection Limit (fg/L)	% Detection (Tropical Atlantic)	% Detection (North Atlantic)
Hexachlorobenzene	17	5.0	15	95	100	100
α-hexachlorocyclohexane	6.5	3.0	8.9	14157	0	0
β-hexachlorocyclohexane	11	2.5	7.5	47516	0	0
γ-hexachlorocyclohexane	20	6.6	20	19894	0	10
δ-hexachlorocyclohexane	26	0.51	1.5	2437	0	0
Heptachlor	11	0.29	0.87	14	0	0
Aldrin	83	11	33	417	0	0
Heptachlor-epoxide	11	12	35	689	0	0
Trans- chlordane	6.4	7.1	21	135	60	10
o,p'-DDE	1.9	0.35	1.1	3.4	30	0
Cis- chlordane	20	1.4	4.2	26	70	20
Endosulfan I	84	55	166	5258	0	0
Trans- nonachlor	18	5.3	16	33	40	0
p,p'-DDE	5.9	1.5	4.6	14	90	100
Dieldrin	127	86	257	16236	0	0
o,p'-DDD	5.7	2.7	8.1	64	40	80
Endrin	181	178	533	6714	0	0
Endosulfan II	155	105	316	125999	0	0
PP-DDD/OP-DDT	5.4	1.7	5.0	50	80	100
Endrin Aldehyde	86	3.5	10.6	666	0	0
Endosulfan sulfate	42	27	81	202987	0	0
p,p'-DDT	17	13	39	66	60	60
Endrin ketone	70	57	170	679	0	0
Methoxychlor	12	2.9	8.8	44	0	0

Table S3. Cont'd. Detection limit of BDEs for mooring samplers.

Compound	Average Field Blank Concentration(ng/g PE)	STDEV	Detection Limit (ng/g PE)	Detection Limit (fg/L)	% Detection (Tropical Atlantic)	% Detection (North Atlantic)
BDE-2	5.3	3.1	9.2	265	0	0
BDE-8	8.6	9.2	27.7	215	0	0
BDE-15	8.6	4.6	13.8	109	0	0
BDE-30	6.1	1.1	3.3	6.9	0	10
BDE-28	13	0.2	0.6	1.3	0	10
BDE-49	3.4	2.9	8.7	7.5	20	0
BDE-47	77	24.5	73.6	62	40	10
BDE-100	31	0.7	2.0	1.3	30	50
BDE-99	81	1.4	4.2	2.6	40	100
BDE-154	36	37.9	113.6	65	10	0
BDE-153	14	8.2	24.7	14	10	0
BDE-183	26	18.8	56.4	31	20	0

Table S3. Cont'd. Detection limit of PAHs for mooring samplers.

Compound	Average Field Blank Concentration(ng/g PE)	STDEV	Detection Limit (ng/g PE)	Detection Limit (pg/L)	% Detection (Tropical Atlantic)	% Detection (North Atlantic)
Biphenyl	1617.5	1038.0	3113.9	985	20	0
Acenaphthylene	117.1	122.1	366.4	116	40	0
Acenaphthene	425.1	395.0	1184.9	298	10	0
Fluorene	561.9	248.9	746.7	94	10	0
Phenanthrene	1338.7	217.1	651.4	41	40	0
Anthracene	1337.2	212.7	638.2	40	0	0
Fluoranthene	340.1	392.0	1176.1	15	70	80
Pyrene	499.6	285.4	856.2	11	40	70
Retene	68.3	49.2	147.6	0	20	20
Benz[a]anthracene	48.8	54.8	164.5	0	90	100
Chrysene	52.1	41.5	124.4	0	90	100
Benzo[b]fluoranthene	527.8	738.0	2214.1	2	10	0
Benzo[k]fluoranthene	1945.6	2694.6	8083.7	7	10	0

Table S4. Recoveries for surrogates in this study.

	Tropical Atlantic				North Atlantic				Atlantic 2010				Pacific 2012				Pacific 2010			
	Min	Max	Mean	Stdev	Min	Max	Mean	Stdev	Min	Max	Mean	Stdev	Min	Max	Mean	Stdev	Min	Max	Mean	Stdev
$^{13}C_{12}$-CB8	17	47	34	9	32	53	46	6	42	92	56	13	33	127	50	20	46	63	53	5
$^{13}C_{12}$-CB28	24	91	61	19	33	68	54	9	6	167	70	28	50	137	70	18	43	55	48	3
$^{13}C_{12}$-CB52	22	60	46	12	40	88	66	13	49	99	69	13	82	141	111	15	32	49	40	4
$^{13}C_{12}$-CB118	26	64	51	13	43	83	63	10	46	109	72	15	41	97	70	14	39	48	44	3
$^{13}C_{12}$-CB138	27	67	54	13	43	84	63	11	50	80	64	8	34	73	61	9	39	48	44	3
$^{13}C_{12}$-CB180	27	69	56	14	47	89	67	12	56	91	70	8	31	88	59	11	31	40	36	2
$^{13}C_{12}$-CB209	16	66	44	14	39	70	54	9	44	82	61	10	32	113	61	15	22	29	25	2
$^{13}C_{6}$-HCBz	15	49	32	11	34	59	48	7	36	80	53	11	30	105	43	16	15	20	17	1
$^{13}C_{12}$-p,p'-DDT	20	65	48	15	35	76	57	11	45	84	65	10	40	112	64	14	32	42	33	11
$^{13}C_{12}$-BDE28	25	69	53	14	34	78	51	12	47	79	62	7	52	72	64	5	69	82	77	4
$^{13}C_{12}$-BDE47	27	80	54	15	37	86	54	16	38	84	63	9	60	111	72	11	69	103	79	10
$^{13}C_{12}$-BDE99	20	70	42	13	27	70	43	14	41	89	57	10	64	105	78	9	60	125	75	16
$^{13}C_{12}$-BDE153	24	81	48	15	22	63	41	13	49	87	65	9	62	86	75	7	59	95	69	9
$^{13}C_{12}$-BDE183	19	65	35	12	15	46	29	9	42	76	58	9	48	76	64	8	56	91	66	9
*d*10-acenaphthene	18	84	46	20	28	50	38	7	33	108	64	20	27	128	54	25	51	446	105	112
*d*10-phenanthrene	37	117	86	25	64	105	88	11	42	132	80	27	37	202	63	41	58	665	200	159
*d*12-chrysene	39	140	103	33	67	122	93	19	57	160	98	31	55	234	78	42	56	230	98	41
*d*12-perylene	7	46	28	13	26	142	53	29	0	61	11	19	55	189	96	39	73	523	115	123

Table S5. Correlation of Rs with measured currents.

	Scenario 1		Scenario 2		Scenario 3		Scenario 4		Scenario 5		Scenario 6	
	Correlation coefficient	p-value	Correlation coefficient	p-value	Correlation coefficient	p-value	Correlation coefficient	p-value	Correlation coefficient	p-value	Correlation coefficient	p-value
					Tropical Atlantic							
800 µm PEs	0.84	0.44	0.94	0.05	0.9	0.05	0.74	0.05	0.94	0.05	0.94	0.05
1600/50 µm PEs	0.04	0.52	0.22	0.49	0.004	0.95	-0.23	0.95	-0.45	0.55	-0.46	0.55
					North Atlantic							
800 µm PEs	0.829	0.33	0.829	0.33	0.37	0.75	-0.96	0.92	-0.83	0.33	-0.83	0.75
1600 µm PEs	-0.88	0.33	-0.88	0.33	-0.83	0.33	-0.92	0.33	-0.86	0.33	-0.86	0.33

Table S6. Derived Rs ratio under each scenario.

	Tropical Atlantic					North Atlantic			
	Rs (800 m)	Rs (1600 m)	Ratio	Average		Rs (800 m)	Rs (1600 m)	Ratio	Average
Scenario 1	100	57	1.8		Scenario 1	38	8	4.8	
	100	26				22	8	2.8	
	100	56	1.8	1.8		42	11	3.8	3.5
	7	4				28	8	3.5	
	28	15	1.9			36	13	2.8	
Scenario 2	50	30	1.7		Scenario 2	38	8	4.8	
	50	12				22	8	2.8	
	24	12	2	1.8		42	11	3.8	3.5
	7	4				28	8	3.5	
	28	15	1.9			36	13	2.8	
Scenario 3	40	24	1.7		Scenario 3	38	8	4.8	
	40	9				22	8	2.8	
	24	12	2	1.8		30	10	3	3.4
	7	4				28	8	3.5	
	28	15	1.9			36	13	2.8	

Table S6. Cont'd. Derived Rs ratio under each scenario.

	Tropical Atlantic					North Atlantic			
	Rs (800 m)	Rs (1600 m)	Ratio	Average		Rs (800 m)	Rs (1600 m)	Ratio	Average
Scenario 4	30	18	1.7		Scenario 4	24	7	3.4	
	30	7				22	8	2.8	
	24	12	2	1.8		30	10	3	3
	7	4				28	8	3.5	
	28	15	1.9			29	12	2.4	
Scenario 5	20	11	1.8		Scenario 5	17	6	2.8	
	20	5				17	7	2.4	
	20	11	1.8	1.8		19	8	2.4	2.5
	7	4				16	6	2.7	
	20	11	1.8			20	10	2	
Scenario 6	10	6	1.7		Scenario 6	10	4	2.5	
	10	5				8	4	2	
	10	6	1.7	1.7		10	5	2	2.1
	7	4				9	4	2.3	
	10	6	1.7			10	6	1.7	

Table S7. Equilibrium reached under Rs/2 and 2*Rs compared to Equilibrium reached under Rs (used in the context)

Rs/2						2*Rs					
PCBs	213 m	468 m	1173 m	1736 m	2535 m	PCBs	213 m	468 m	1173 m	1736 m	2535 m
8	1.1	1.2	1.2	1.3	1.2	8	1	0.9	1	1	1
18	1.5	1.6	1.5	1.7	1.5	18	0.8	0.8	0.8	0.8	0.8
28	1.8	1.8	1.8	2	1.8	28	0.6	0.6	0.6	0.6	0.6
52	1.9	1.9	1.9	2.1	1.9	52	0.6	0.5	0.6	0.5	0.6
44	1.8	1.9	1.8	2.1	1.8	44	0.6	0.6	0.6	0.6	0.6
66	1.9	2	1.9	2.2	1.9	66	0.5	0.5	0.5	0.5	0.5
101	2	2	2	2.2	2	101	0.5	0.5	0.5	0.5	0.5
118	2	2	2	2.2	2	118	0.5	0.5	0.5	0.5	0.5
105	2	2	2	2.2	2	105	0.5	0.5	0.5	0.5	0.5
153	2	2	2	2.2	2	153	0.5	0.5	0.5	0.5	0.5
138	2	2	2	2.2	2	138	0.5	0.5	0.5	0.5	0.5
206	2	2	2	2.2	2	206	0.5	0.5	0.5	0.5	0.5
209	2	2	2	2.2	2	209	0.5	0.5	0.5	0.5	0.5
Maximum			2.2			Minimum			0.5		

Table S8. %Equilibrium for PCBs, OCPs, PBDEs and PAHs from the Tropical Atlantic.

	800 um PEs					1600 & 50 um PEs				
	26 m	84 m	251 m	800 m	1800 m	26 m	84 m	251 m	800 m	1800 m
PCB 8	100	100	100	97	98	99	100	98	100	88
PCB 11	97	98	94	74	78	85	100	77	100	55
PCB 18	98	99	95	77	80	87	100	79	100	57
PCB 28	70	74	62	37	40	47	99	39	86	24
PCB 52	46	49	38	21	23	27	89	22	63	13
PCB 44	62	65	53	31	33	40	97	33	79	19
PCB 66	26	29	21	11	12	15	66	12	39	7
PCB 101	14	15	11	6	6	8	42	6	22	3
PCB 118	11	13	9	4	5	6	35	5	18	3
PCB 105	11	13	9	4	5	6	35	5	18	3
PCB 153	5	5	4	2	2	3	16	2	8	1
PCB 138	3	3	2	1	1	2	10	1	5	1
PCB 128	7	8	6	3	3	4	24	3	12	2
PCB 187	2	3	2	1	1	1	8	1	4	1
PCB 180	2	3	2	1	1	1	8	1	4	1

Table S8. Cont'd. %Equilibrium for PCBs, OCPs, PBDEs and PAHs from the Tropical Atlantic.

	800 um PEs					1600 & 50 um PEs				
	26 m	84 m	251 m	800 m	1800 m	26 m	84 m	251 m	800 m	1800 m
Hexachlorobenzene	85	88	78	52	56	64	100	55	96	35
o,p'-DDE	70	74	62	37	40	47	99	39	86	24
p,p'-DDE	62	65	53	31	33	40	97	33	79	19
Trans- chlordane	85	88	78	52	56	64	100	55	96	35
Cis- chlordane	85	88	78	52	56	64	100	55	96	35
Trans- nonachlor	46	49	38	21	23	27	89	22	63	13
o,p'-DDD	91	93	85	60	64	72	100	63	98	42
p,p'-DDT / o,p'-DDT	62	65	53	31	33	40	97	33	79	19
p,p'-DDT	38	41	32	17	18	22	82	18	55	10
BDE 47	14	15	11	6	6	8	42	6	22	3
BDE 100	4	4	3	1	2	2	13	2	6	1
BDE 99	4	4	3	1	2	2	13	2	6	1
Acenaphthylene	100	100	100	100	100	100	100	100	100	100
Phenanthrene	100	100	100	100	100	100	100	100	100	98
Fluoranthene	97	98	94	73	77	84	100	76	100	54
Pyrene	97	98	94	73	77	84	100	76	100	54
Benzo(a)anthracene	50	54	42	23	26	31	92	25	68	14
Chrysene	50	54	42	23	26	31	92	25	68	14
Benzo(b)fluoranthene	16	18	13	6	7	9	47	7	25	4

Table S9. %Equilibrium for PCBs, OCPs, PBDEs and PAHs from the North Atlantic.

	800 µm PEs					1600 µm PEs				
	213 m	468 m	1173 m	1736 m	2535 m	213 m	468 m	1173 m	1736 m	2535 m
PCB 18	78	69	74	70	76	44	40	45	37	50
PCB 28	38	31	35	32	36	17	15	17	14	20
PCB 52	22	17	19	17	20	9	8	9	7	11
PCB 44	32	25	29	26	30	14	12	14	11	16
PCB 101	6	4	5	5	5	2	2	2	2	3
PCB 118	5	4	4	4	4	2	2	2	1	2
PCB 153	2	1	2	2	2	1	1	1	1	1
Hexachlorobenzene	54	44	49	45	51	26	23	26	21	30
p,p'-DDE	32	25	29	26	30	14	12	14	11	16
o,p'-DDD	62	52	57	53	59	31	28	32	26	36
p,p'-DDD / o,p'-DDT	32	25	29	26	30	14	12	14	11	16
p,p'-DDT	18	14	16	14	16	7	6	7	6	8
BDE 100	1	1	1	1	1	1	0.5	1	0.5	1
BDE 99	1	1	1	1	1	1	0.5	1	0.5	1
Fluoranthene	75	65	71	67	72	41	37	42	35	47
Pyrene	75	65	71	67	72	41	37	42	35	47
Benzo(a)anthracene	24	19	22	20	23	10	9	10	8	12
Chrysene	24	19	22	20	23	10	9	10	8	12

Table S10. Deviation of detected concentrations between PEs from the same cages.

	Tropical Atlantic						North Atlantic				
	26 m	84 m	251 m	800 m	1800 m		213 m	468 m	1173 m	1736 m	2535 m
PCB 8	123	112	34	108	27	PCB 18	82	4	74	8	92
PCB 18	9	37	13	74	25	PCB 28	140	3	19	9	96
PCB 28	109	128	121	3	27	PCB 52	8	18	27	59	44
PCB 52	117	13	72	70	7	PCB 44	8	0	36	9	42
PCB 44	105	29	87	69	21	PCB 101	7	23	63	78	8
PCB 66	81	129	92	137	116	PCB 118	140	140	140	141	47
PCB 101	31	94	22	85	4	PCB 153	120	9	134	122	47
PCB 118	22	79	11	36	7	Hexachlorobenzene	4	2	3	1	3
PCB 105	19	140	7	28	4	p,p'-DDE	44	13	4	1	5
PCB 153	5	52	13	12	7	o,p'-DDD	89	97	12	32	1
PCB 138	2	87	1	23	5	p,p'-DDT / o,p'-DDT	68	36	5	2	16
PCB 128	43	79	43	16	44	p,p'-DDT	60	52	28	9	11
PCB 187	15	15	29	43	20	BDE 100	136	138	101	62	135
Hexachlorobenzene	5	40	3	4	14	BDE 99	122	28	23	38	104
o,p'-DDE	28	20	31	26	139	Fluoranthene	3	3	2	6	30
p,p'-DDE	25	136	7	19	6	Pyrene	0	13	2	47	30
Trans- chlordane	54	9	23	126	30	Benzo(a)anthracene	3	13	8	26	5

Table S10. Cont'd. Deviation of detected concentrations between PEs from the same cages.

	Tropical Atlantic					North Atlantic				
	26 m	84 m	251 m	800 m	1800 m	213 m	468 m	1173 m	1736 m	2535 m
Cis- chlordane	18	9	27	139	4					
Trans- nonachlor	35	131	4	127	40					
o,p'-DDD	17	5	95	138	13					
p,p'-DDT / o,p'-DDT	118	139	42	27	11					
p,p'-DDT	78	127	39	5	5					
BDE 47	100	48	42	3	43					
BDE 100	136	134	44	128	44					
BDE 99	139	117	44	123	44					
Acenaphthylene	0	0	0	59	0					
Phenanthrene	0	91	0	0	0					
Fluoranthene	0	0	0	0	1					
Pyrene	10	48	2	6	20					
Benzo(a)anthracene	36	44	119	73	119					
Chrysene	83	10	3	1	0					
Mean	50	68	35	55	27	61	35	40	38	42
Std	47	51	36	50	36	55	46	46	43	41

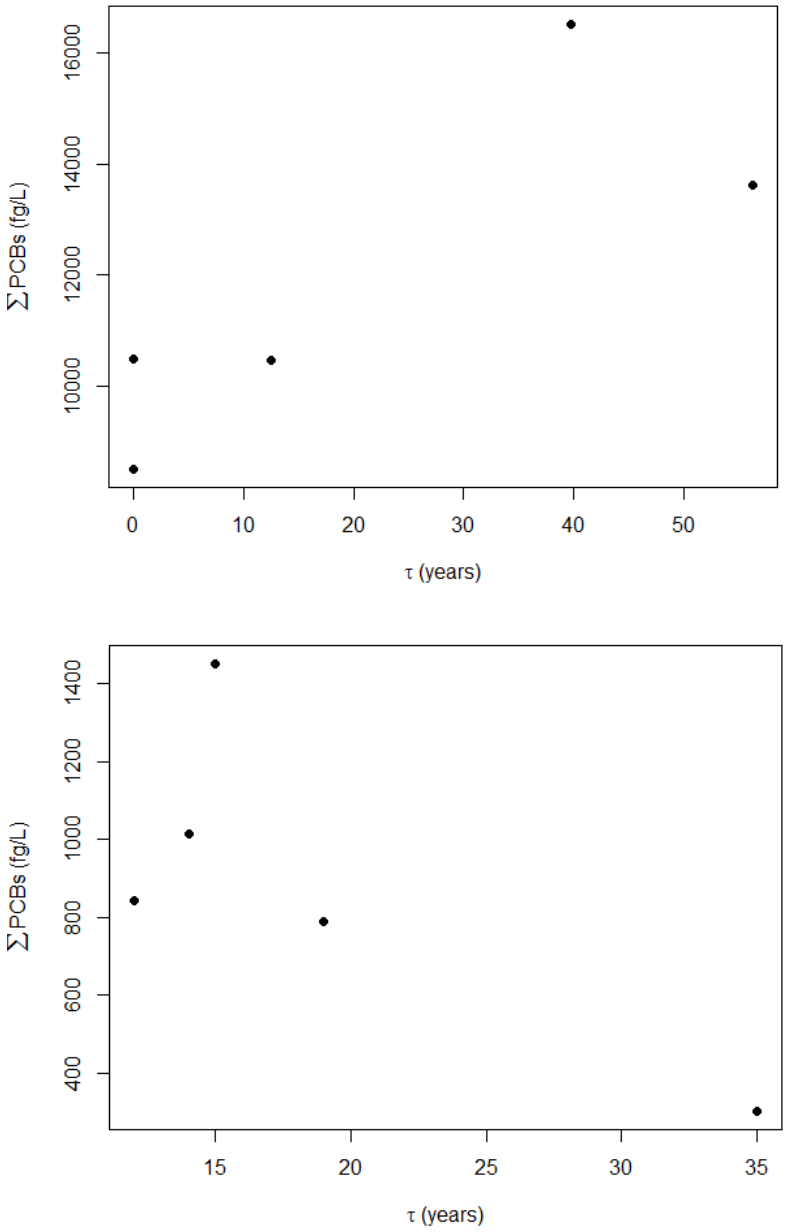

Figure S3. ∑PCBs versus derived ventilation age (τ) for the tropical Atlantic site (top) and the north Atlantic site (bottom).

Table S11. CFC-12 data and derived ventilation age (τ in years) for Tropical Atlantic site.

SITE 1[a] (24.50 ˚ N, -37.70 ˚ E)			SITE 2 [a] (24.50 ˚ N, -38.52 ˚ E)			SITE 3[a] (24.49 ˚ N, -39.24 ˚ E)			PEs		
CFC sampling depth (m)	CFC-12 (χ)	τ (years)	CFC sampling depth (m)	CFC-12 (χ)	τ (years)	CFC sampling depth (m)	CFC-12 (χ)	τ (years)	PE sampling depth (m)	∑PCBs (fg/L)	Averaged CFC-12 (χ)
23	553	-	20	596	-	23	566	-	26	8494	-[b]
64	549	-	61	596	-	63	559	-			
115	558	-	111	591	-	114	555	-	84	10479	-[b]
215	524	11	211	557	-	214	499	14	251	10464	13[c]
366	455	17	362	478	16	365	450	17			
511	361	22	514	409	19	516	368	22			
712	130	35	715	159	33	718	141	34	800	16524	40[c]
921	25	47	918	36	44	919	28	46			
1124	16	50	1120	24	47	1122	17	50			
1377	14	51	1322	20	48	1323	14	51			
1629	8	54	1524	12	52	1577	10	53			
1881	4.3	57	1775	5.9	56	1831	5.9	56	1800	13624	56[c]

a) Original data from EXPOCODE 74DI20040404.
b) Replaced by 0 for plotting Figure S2.
c) Calculated by averaging out τ from similar depths, indicated by same colors.

Table S11. Cont'd. CFC-12 data and derived ventilation age (τ in years) for North Atlantic site.

SITE [a] (77.00 ˚ N, 1.50˚ E)			PEs		
SF6 sampling depth (m)	SF-6 (χ)	τ (years)	PE sampling depth (m)	∑PCBs (fg/L)	Averaged CFC-12 (χ)
10	13	0			
49	5.7	5			
100	4.6	10			
200	4.1	12	213	844	12[b]
300	4.4	11			
400	3.3	16			
501	3.8	14	468	1452	15[b]
601	3.8	14			
800	4.0	13			
1001	5.0	8			
1200	3.8	14	1173	1015	14[b]
1501	4.0	13	1736	789	
2000	1.5	25			19[b]
2500	0.4	35	2535	302	40[b]

a) Original data from EXPOCODE 58GS20090528.

b) Calculated by averaging out τ from similar depths, indicated by same colors.

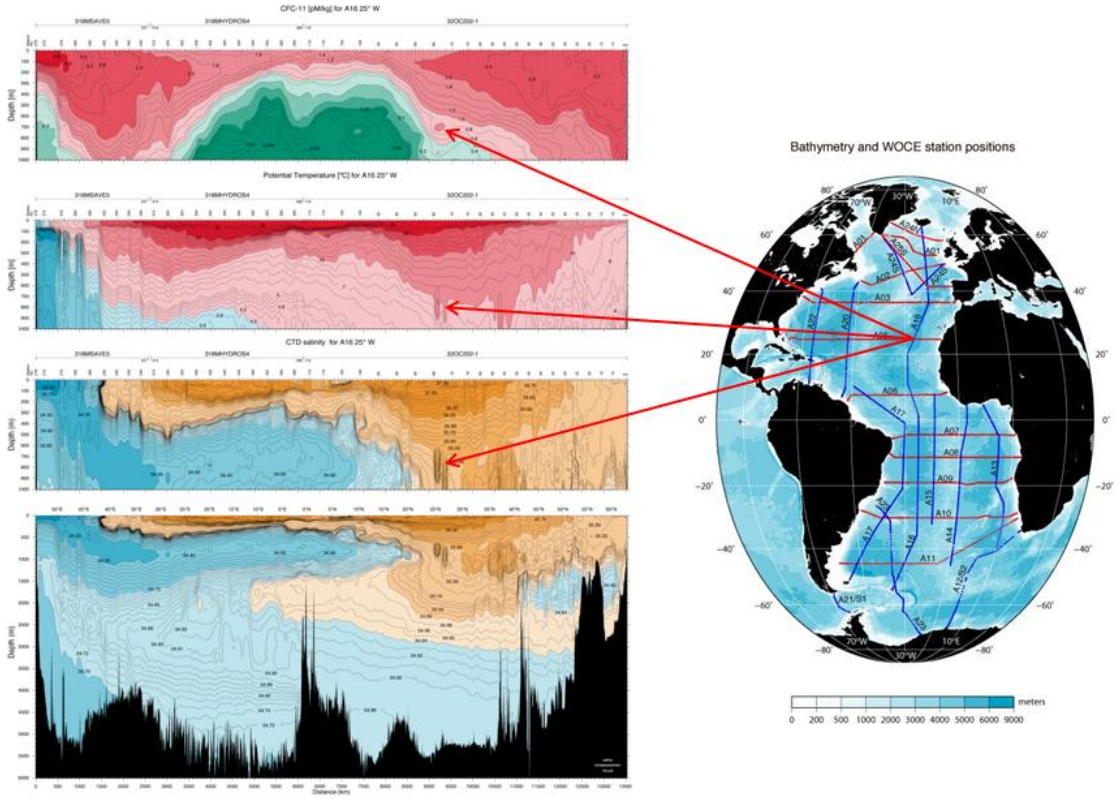

Figure S4. Vertical section of CFC-11 (top), temperature (middle) and salinity (bottom) from A16 WOCE ATLAS (Accessed on June 21, 2015).

Table S12. Sampling information for Pacific SEA Cruise (2012).

Sample No.	Location Deployed	Date Deployed	Time Deployed	Location Recovered	Date Recovered	Time Recovered	Days Deployed	Average Air/Water Temperature (℃)	Wind Speed (knots)	Weight PE (g)	Sampling Rate (L/day)
A-1	32° 37.5' N, 117° 16.1' W	4-Oct-12	11:52	32° 17.9' N, 123° 53.9' W	7-Oct-12	16:00	3	20.75	13.1	2.07	94210
W-1	32° 37.7' N, 117° 17.3' W			32° 18.6' N, 123° 54.2' W				19.5		1.61	31
A-2	32° 17.1' N, 123° 53.7' W	7-Oct-12	16:00	33° 44.2' N, 133° 28.2' W	14-Oct-12	16:00	7	21.75	9.8	2.1	56607
W-2	32° 18.0' W, 123° 54.0' W			33° 44.2' N, 133° 28.2' W				19.9		2.16	35
A-3	33° 44.2' N, 133° 28.2' W	14-Oct-12	16:00	31° 42.4' N, 139° 58.2' W	21-Oct-12	22:30	7	22.1	10.5	1.77	38012
W-3	33° 44.2' N, 133° 28.2' W			31° 42.4' N, 139° 58.2' W				23		1.78	30
A-4	31° 42.4' N, 139° 58.1' W	21-Oct-12	22:00	30° 20.8' N, 145° 40.8' W	28-Oct-12	7:30	6.5	22.95	12.4	2.21	54375
W-4	31° 42.4' N, 139° 58.1' W			30° 20.8' N, 145° 40.7' W				23.6		1.61	23

Table S12. Cont'd. Sampling information for Pacific SEA Cruise (2012).

Sample No.	Location Deployed	Date Deployed	Time Deployed	Location Recovered	Date Recovered	Time Recovered	Days Deployed	Average Air/Water Temperature (℃)	Wind Speed (knots)	Weight PE (g)	Sampling Rate (L/day)
A-5	30˚ 20.8 N, 145˚ 40.6 W	28-Oct-12	7:30	21˚ 23.4' N, 152˚ 01.2' W	4-Nov-12	12:32	7	25.75	9.7	1.75	27278
W-5	30˚ 20.7' N, 145˚ 40.6 W			21˚ 23.4' N, 152˚ 01.2' W				24.9		2.18	38
Engine Room	32˚ 37.7' N, 117˚ 17.3' W	4-Oct-12	12:20	21˚ 23.4' N, 152˚ 01.2' W	4-Nov-12	12:32	31	24.25		2.17	560412
Science Lab	32˚ 37.7' N, 117˚ 17.3' W	4-Oct-12	12:20	21˚ 23.4' N, 152˚ 01.2' W	4-Nov-12	12:32	31	24.25		1.68	85048
Galley	32˚ 37.7' N, 117˚ 18.1' W	4-Oct-12	12:20	21˚ 23.4' N, 152˚ 01.2' W	4-Nov-12	12:32	31	24.25		1.9	68689

Table S13. Sampling information for Pacific SEA Cruise (2010).

Sample No.	Location Deployed	Date Deployed	Time Deployed	Location Recovered	Date Recovered	Time Recovered	Days Deployed	Average Air/Water Temperature (℃)	Wind Speed (knots)	Weight PE (g)	Sampling Rate (L/day)
A-1	21° 47.3'N, 159° 37.1'W	2-Jul-10	13:30	33° 37.3'N, 157° 24.5'W	8-Jul-10	19:40	6	25.1	11.7	1.88	51460
W-1								26.7		1.59	51
A-2	33° 37.3'N, 157° 24.5'W	8-Jul-10	19:40	42° 08.0'N, 138° 23.7'W	16-Jul-10	10:45	7.5	20.3	8.7	1.56	41986
W-2				42° 08.2'N, 138° 32.4'W		9:39		21.7		1.78	47
A-3	42° 08.0'N, 138° 23.7'W	16-Jul-10	10:45	42° 01.0' N, 130° 25.0' W	21-Jul-10	7:30	5.5	15.8	14.3	1.79	127138
W-3	42° 08.2'N, 138° 32.4'W		9:39	40° 38.4'N, 127° 30.6'W	22-Jul-10	0:55	5	15.8		1.88	58
A-4	40° 43.3'N, 127° 39.8'W	22-Jul-10	23:40	32˚ 16.4' N , 64˚24.1' W	26-Jul-10	N/A	4	15	22.9	1.69	102385
W-4	40° 38.4'N, 127° 30.6'W	21-Jul-10	0:55	38° 00.1'N, 122° 57.8'W			5	15.4		1.74	59

Table S17. Cont'd.Sampling information for Pacific SEA Cruise (2010).

Sample No.	Location Deployed	Date Deployed	Time Deployed	Location Recovered	Date Recovered	Time Recovered	Days Deployed	Average Air/Water Temperature (℃)	Wind Speed (knots)	Weight PE (g)	Sampling Rate (L/day)
Engine Room		16-Jul-10	10:55		30-Jul-10	9:45	14	17		1.67	20950
Galley		21-Jul-10	7:45		30-Jul-10	9:30	9	15.5		1.66	195400

Table S14. Detection limit of PCBs for Pacific SEA Cruise samplers (2012).

Compound	Average Field Blank Concentration(pg/g PE)	STDEV	Detection Limit (pg/g PE)	Detection Limit Air Samples (pg/m3)	Detection Limit Water Samples (pg/L)	% Detection (True Samples)	% Detection (Ship Background)
PCB 8	237	34.1	102.3	28.2	3.4	30	33
PCB 11	56	8	23	1.8	0.4	30	100
PCB 18	65	16.59	49.8	5.3	0.9	20	67
PCB 28	159	47.71	143.13	6.7	1.7	10	67
PCB 44	216	196.0	588	17.1	6.9	0	33
PCB 52	65	14	41	0.9	0.4	0	0
PCB 66	12.5	9.9	30	0.4	0.3	0	67
PCB 81	6	4.2	12.6	0.1	0.1	0	0
PCB 77	6	4	12	0.1	0.1	0	67
PCB 101	13	11.4	34.2	0.3	0.4	90	0
PCB 118	39.1	25.962	77.89	0.5	0.8	0	0
PCB 123	22.2	16.23	48.70	0.4	0.5	60	67
PCB 114	26.1	22.80	68.40	0.5	0.7	0	0
PCB 105	62	27.4	82.1	0.5	0.8	0	0
PCB 126	24	31.6	94.9	0.6	1.0	0	0
PCB 153	11.8	6.47	19.4	0.1	0.2	70	0
PCB 138	13.7	16.6	50	0.3	0.5	40	0
PCB 128	14	8	24	0.2	0.2	20	0
PCB 167	10	10	29	0.2	0.3	0	33
PCB 156	18.6	18.8	57	0.4	0.6	0	67
PCB 157	9	8	23	0.1	0.2	0	0
PCB 169	19	11	33	0.2	0.3	70	33
PCB 187	41	31	93	0.6	0.9	20	0
PCB 180	31	27.5	82	0.5	0.8	0	33
PCB 170	28	27	82	0.5	0.8	30	67
PCB 189	15	8	23	0.1	0.2	60	67
PCB 195	95	60.1	180	1.1	1.8	0	0
PCB 206	171	79.0	237.1	1.4	2.4	0	0
PCB 209	90.5	51.19	153.6	0.9	1.5	0	0

a) Estimated typical ambient detection limit using deployment time 6.1 days, sampler mass 2.1 g, and mean air sampling rates (54096 L/day) and mean water sampling rate (31 L/day). **b)** Pacific cruise(2010) detection limit was close to (2012), thus only DL from 2012 was shown.

Table S14. Cont'd. Detection limit of OCPs for Pacific SEA Cruise samplers (2012).

Compound	Average Field Blank Concentration(pg/g PE)	STDEV	Detection Limit (pg/g PE)	Detection Limit Air Samples (pg/m3)	Detection Limit Water Samples (pg/L)	% Detection (True Samples)	% Detection (Ship Background)
Hexachlorobenzene	134	55.0	164.9	32.9	2.2	100	100
α-hexachlorocyclohexane	77	7.9	23.8	9.5	37.8	70	100
β-hexachlorocyclohexane	12	6.3	19.0	1.9	120.1	0	0
γ-hexachlorocyclohexane	72	12.9	38.8	3.1	38.8	80	100
δ-hexachlorocyclohexane	34	16.6	49.8	1.3	78.9	20	67
Heptachlor	13	8.2	24.5	6.2	0.5	0	0
Aldrin	7	4.2	12.7	1.6	0.2	0	0
Heptachlor-epoxide	5	1.7	5.2	0.1	0.1	0	0
Trans- chlordane	12	4.9	14.7	0.3	0.2	10	33
o,p'-DDE	82	73.4	220.3	1.91	2.58	0	0
Cis- chlordane	16	13.3	39.8	0.6	0.5	20	33
Endosulfan I	5	2.9	8.8	0.1	0.3	0	0
Trans- nonachlor	20	7.2	21.6	0.1	0.2	0	0
p,p'-DDE	69	40.9	122.7	1.1	1.4	0	0
Dieldrin	5	2.8	8.4	0.2	0.5	0	0
o,p'-DDD	344	226.7	680.2	4.5	9.9	0	0
Endrin	8	4.8	14.5	0.1	0.3	0	0
Endosulfan II	3	1.5	4.4	0.0	1.7	0	0
PP-DDD/OP-DDT	296	148.4	445.1	3.1	7.1	0	0
Endrin Aldehyde	1	0.4	1.3	0.0	0.1	0	0
Endosulfan sulfate	7	5.6	16.8	0.1	42.3	10	33
p,p'-DDT	65	28.5	85.4	0.5	0.9	20	33
Endrin ketone	3	2.3	7.0	0.0	0.1	0	0
Methoxychlor	27	29.6	88.7	0.5	1.1	0	0

Table S14. Cont'd. Detection limit of BDEs for Pacific SEA Cruise samplers (2012).

Compound	Average Field Blank Concentration(pg/g PE)	STDEV	Detection Limit (pg/g PE)	Detection Limit Air Samples (pg/m3)	Detection Limit Water Samples (pg/L)	% Detection (True Samples)	% Detection (Ship Background)
BDE-2	4	3.8	11.5	1.0	0.4	0	0
BDE-8	7	5.7	17.0	0.2	0.2	0	67
BDE-15	3	1.8	5.4	0.1	0.1	10	67
BDE-30	10	9.9	29.6	0.2	0.3	0	0
BDE-28	19	10.2	30.6	0.2	0.3	70	100
BDE-49	11	9.8	29.4	0.2	0.3	0	0
BDE-47	214	55.5	166.4	1.0	1.7	80	67
BDE-100	44	23.7	71.0	0.4	0.7	40	67
BDE-99	76	22.5	67.6	0.4	0.7	100	100
BDE-154	98	56.8	170.3	1.0	1.7	20	67
BDE-153	17	31.6	94.9	0.6	1.0	10	100
BDE-183	42	17.4	52.1	0.3	0.5	10	33

Table S14. Cont'd. Detection limit of PAHs for Pacific SEA Cruise samplers (2012)

Compound	Average Field Blank Concentration(pg/g PE)	STDEV	Detection Limit (pg/g PE)	Detection Limit Air Samples (pg/m3)	Detection Limit Water Samples (pg/L)	% Detection (True Samples)	% Detection (Ship Background)
Biphenyl	4329	1695	5086	4439	1608	0	0
Acenaphthylene	811	376	1128	1561	357	0	33
Acenaphthene	1438	464	1391	1529	350	20	33
Fluorene	1778	391	1173	513	148	30	100
Phenanthrene	3581	1193	3578	393	226	50	100
Anthracene	501	107	322	22	20	40	100
Fluoranthene	365	88	265	3	5	90	100
Pyrene	980	150	449	5	8	90	100
Retene	183	166	497	3	6	30	100
Benz[a]anthracene	175	109	327	2	4	10	67
Chrysene	140	72	216	1	2	50	100
Benzo[b]fluoranthene	43	19.2	57.5	0.3	0.6	20	67
Benzo[k]fluoranthene	25	22.7	68.0	0.4	0.7	20	67

BDEs and PAHs air-water exchange fluxes for Pacific cruises

BDEs

Fluxes in this study were dominated by BDE-47, 99, 100 and were as large as -5.6 ± 2.8 ng m^{-2} day^{-1} (BDE-99). BDE-209 was not measured due to instrument limitation. The fluxes for BDE-47 from Pacific 2010 cruise was high (-5.5 ± 2.8 ng m^{-2} day^{-1}) compared to the measurement form Pacific 2012 at lower latitude (-0.03 ± 0.02 ng m^{-2} day^{-1}). The latter measurement was close to a flux of <0.18 ng m^{-2} day^{-1} from a cruise starting Northeast Asia to the Arctic (Möller et al., 2011).

PAHs

There were large variations regarding the PAHs fluxes. Pacific 2010 cruise had much larger PAHs fluxes (acenapthene: -127 ± 65 ng m^{-2} day^{-1}). In spite of a different compound, a net deposition of 70-210 ng m^{-2} day^{-1} (phenanthrene) was reported by (Nizzetto et al., 2008) that is at the same magnitude as acenapthene flux from our study.

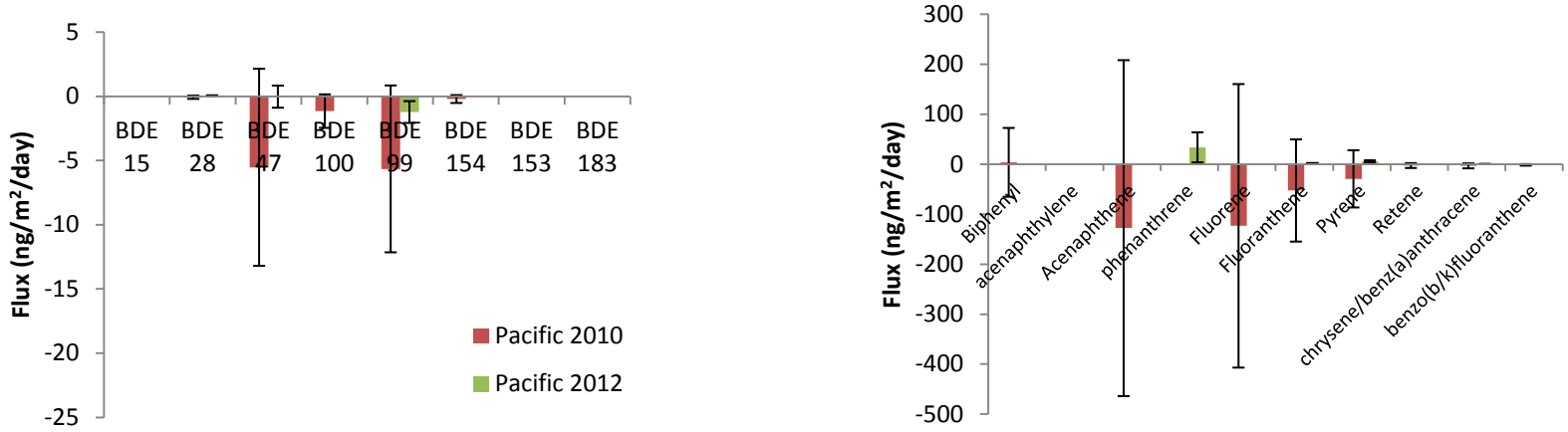

Figure S5. Averaged air-water exchange fluxes of BDEs and PAHs from the two cruises.

Error bars represent standards deviation between samples from each cruise.

An additional cruise - Atlantic 2010

There was one cruise in the Atlantic that started near Bermuda in mid June 2010 and then headed towards the mid-ocean ridge and finally returned to Bermuda in mid July 2010. The air and water samples collected were marked on Figure 2.1. The numbers on the figure represented the order of samples taken. For each number, there were one air and one water sample collected. In addition, in order to check the background contamination from the ship, PEs were deployed in the lab, engine room and galleys on the ship.

Detected POPs Concentration

Concentrations were biased high, and therefore the discussion of this cruise was not the focus in the main context but only mentioned here.

PCB-11 and 118 were the only two congeners detected in the Atlantic cruise, with PCB-11 at much higher concentrations averaging 40 pg m^{-3} while PCB-118 below 5 pg m^{-3}. The mean concentration of PCB-118 from this study (0.7 pg m^{-3}) is slightly smaller than the measurement (1.5 pg m^{-3}) by Jones et al. (2004) and (2.5 pg m^{-3}) by Gioia et al. (2008b) near the west coast of Africa.

Dissolved concentration of PCB-11 and 118 were near 7 pg L^{-1} and 1 pg L^{-1}, respectively. Measurements of dissolved PCB-118 (0.04 pg L^{-1}) from Gioia et al. (2008b) and (0.04-0.1 pg L^{-1}) from Lohmann et al. (2012b) were both 10 times smaller than from this study.

HCB was the only detected OCPs, with a mean concentration of 180 pg m^{-3}. Lower concentration was reported by other studies: 23 pg m^{-3} from Jones et al. (2004), 55 pg m^{-3} from Barber et al. (2005) and 4.4 pg m^{-3} from Lohmann et al. (2012b).

HCB dissolved phase was at a mean concentration of 12 pg L^{-1}; comparable to the northern hemisphere average of 12 pg L^{-1} (Barber et al., 2005).

BDE-47, 99 were the most abundant congeners, averaging 100 and 50 pg m^{-3} respectively in the air. Lower values were reported from other studies: 1-8 pg m^{-3} (BDE 47) and < 4 pg m^{-3} (BDE 99) by Lohmann et al. (2013); < 2.27 pg m^{-3} (BDE 47) and < 0.53 pg m^{-3} (BDE 99) by Xie et al. (2011).

Similar case was found with dissolved BDEs, with concentration from this study at 30 and 20 pg L^{-1} respectively for BDE-47 and 99; higher than 0.5 pg L^{-1} (BDE 47) and < 0.1 pg L^{-1} (BDE 99) by Lohmann (2013a); < 1.05 pg L^{-1} (BDE 47) and < 0.53 pg L^{-1} (BDE 99) by Xie et al. (2011).

Acenaphthylene, Chrysene/Benzo(a)anthracene and Benzo(b/k)fluoranthene were the only three detected PAHs. The averaged air concentration were 250, 28 and 2 pg m^{-3}; dissolved concentration were 80, 30 and 1.5 pg L^{-1}.

Comparison between Atlantic and Pacific, 2010

There were fewer PCBs congeners and OCPs but more BDEs congeners detected in the Atlantic. Due to the enormous difference in acenaphthene and fluorene from literature data in the Pacific cruise, conclusions were hard to make whether the samples were representative of PAHs in the open Pacific ocean.

Table S7 gave the p-value for all the comparisons of both representative compound from each group (PCB-11, HCB, BDE-47 and crysene/benzo(a)znthracene) and the sum of each group (∑PCB, ∑OCP,∑BDE, ∑PAH) between the two basins. The significant differences between the two cruises lied in the same pattern in the atmosphere and water, such that significant difference in the air resulted in also significant difference in the water. This consistency in the POPs distribution within each basin suggesting little contact of air/water between the basins and

undergoing air-water exchanges within each basin. Dissolved phase ∑OCP difference was mainly from the ∑HCHs that were only detected in the Pacific. It was pointed out that HCHs were still in use in developing countries such as China and India, while banned for decades in most of the industrialized countries (Kallenborn et al. 2007). Due to the limited transportation between the basins, it is not surprising to see HCHs only being detected in the Pacific.

Gradients

The detailed gradient values for this cruise was given in Table S22. Similar patterns were shown as Pacific 2010 cruise, such that most PCBs and OCPs favored evaporation/equilibrium while BDEs favored deposition and PAHs favored deposition/equilibrium.

Fluxes

The overall air-water exchange fluxes of PCBs for the Atlantic cruise was small (~0.08 ng m^{-2} day^{-1}), smaller range than fluxes in the Atlantic (-7 - 0.02 ng m^{-2} day^{-1}) (Gioia et al.,2008b), Pacific Ocean (0.5 - 30 ng m^{-2} day^{-1})(Zhang & Lohmann, 2010).

An averaged flux for HCB was between 0.8 ng m^{-2} day^{-1}. Volatilization/equilibrium of HCB was found in the tropical Atlantic (Lohmann et al., 2012b); equilibrium was found in the North Atlantic (Lohmann et al., 2009) and the Pacific (Zhang & Lohmann, 2010).

BDEs favored deposition in all samples. Fluxes in this study were dominated by BDE-47, 99, 100 and were as large as -13 ng m^{-2} day^{-1} (BDE-47) due to the large concentration detected either in the air or water. For all congeners, Atlantic samples yielded larger deposition fluxes than Pacific samples. The absolute flux for BDE-47 from the Atlantic cruise (-13 ng m^{-2} day^{-1}) was more than 10 times higher than (<492 ng m^{-2} day^{-1})(Möller et al., 2011), (median: 83 pg m^{-2} day^{-1})(Xie et al., 2011) and (~ 320 ng m^{-2} day^{-1}) (Lohmann et al., 2013a). It could not be ruled out that contamination occurred during the Atlantic cruise. The overall PAHs fluxes for the Atlantic cruise were small, with a total flux of -6 ng m^{-2} day^{-1}. There were no significant differences in fluxes between the basins.

Table S15. Sampling information for Atlantic SEA Cruise (2010).

Sample No.	Location Deployed	Date Deployed	Time Deployed	Location Recovered	Date Recovered	Time Recovered	Days Deployed	Average Air/Water Temperature (℃)	Wind Speed (knots)	Weight PE (g)	Sampling Rate (L/day)
A-1	32° 10.6' N, 60° 38.2' W	13-Jun-10	8:00	32° 08.5' N , 45°44.2' W	19-Jun-10	17:00	6.50	25.15	10.4	1.82	24768
W-1								24.45		1.66	26
A-2	32° 08.5' N, 45°44.2' W	19-Jun-10	17:00	27° 56.7' N, 44°29.8' W	27-Jun-10	16:20	8	27.65	12.9	1.65	12375
W-2								25.25		1.60	16
A-3	27° 56.7' N ,44°29.8' W	27-Jun-10	16:20	26° 50' N , 49° 57' w	3-Jul-10	17:00	6	27	14.4	1.72	15806
W-3								25.85		1.55	16
A-4	26° 50' N , 49° 57.0' w	3-Jul-10	17:00	32° 16.4' N , 64°24.1' W	13-Jul-10	1:00	8.5	26.75	12.3	1.77	16748
W-4								26.6		1.65	22
Lab Background-1	32° 10.6' N, 60° 38.0' W	13-Jun-10	9:00	32° 08.5' N , 45°44.2' W	19-Jun-10	17:00	6.5	25.15		2.00	40993
Lab Background-2	32° 08.5' N ,45°44.2' W	19-Jun-10	17:00	32° 16.4' N, 64°24.1' W	13-Jul-10	1:00	27.4	26		1.87	7469
Engine Room										1.88	91404
Galley										1.88	68468

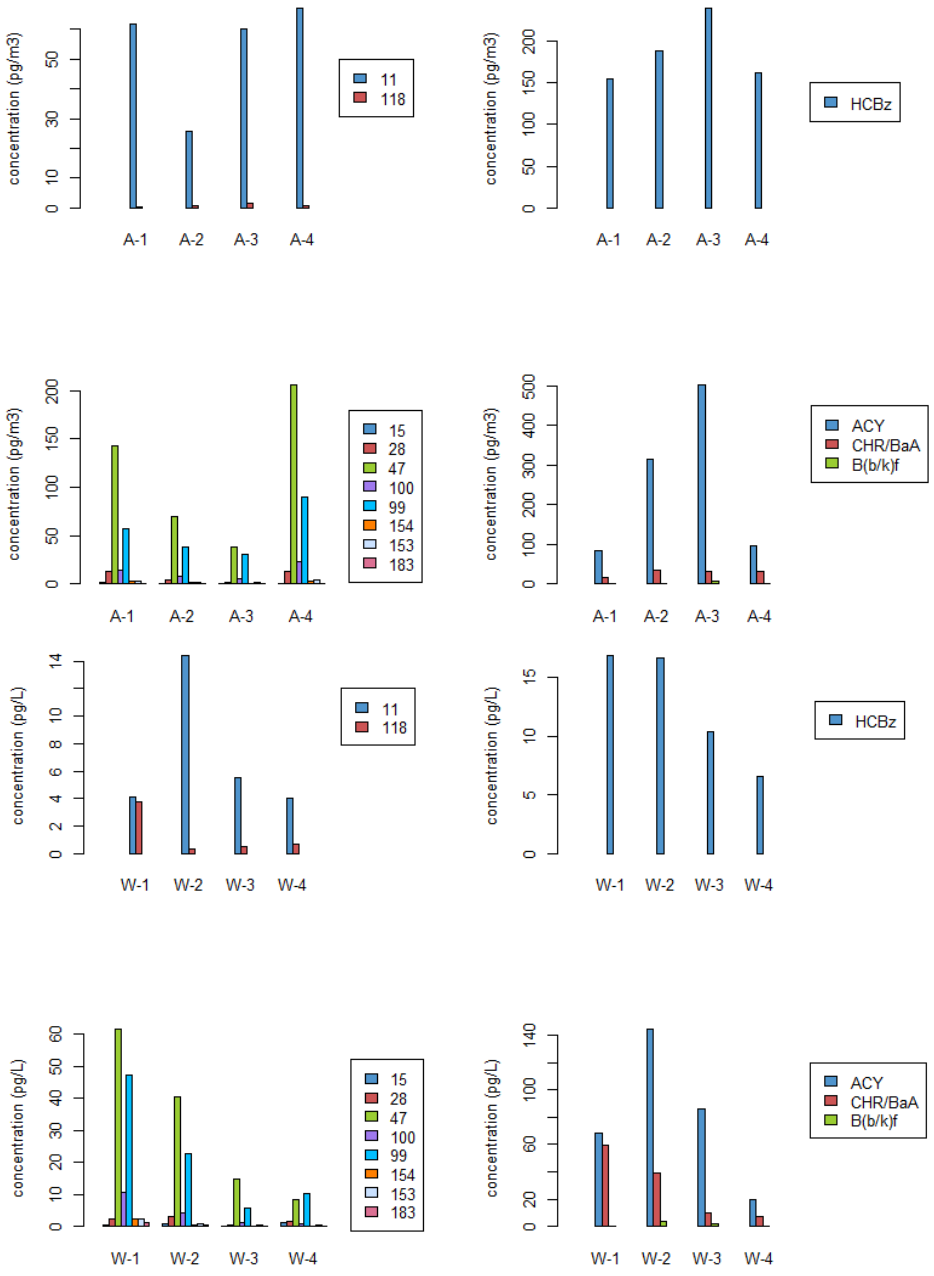

Figure S6. Atmospheric (top) and dissolved (bottom) concentrations of PCBs, OCPs, BDEs and PAHs in the Atlantic 2010.

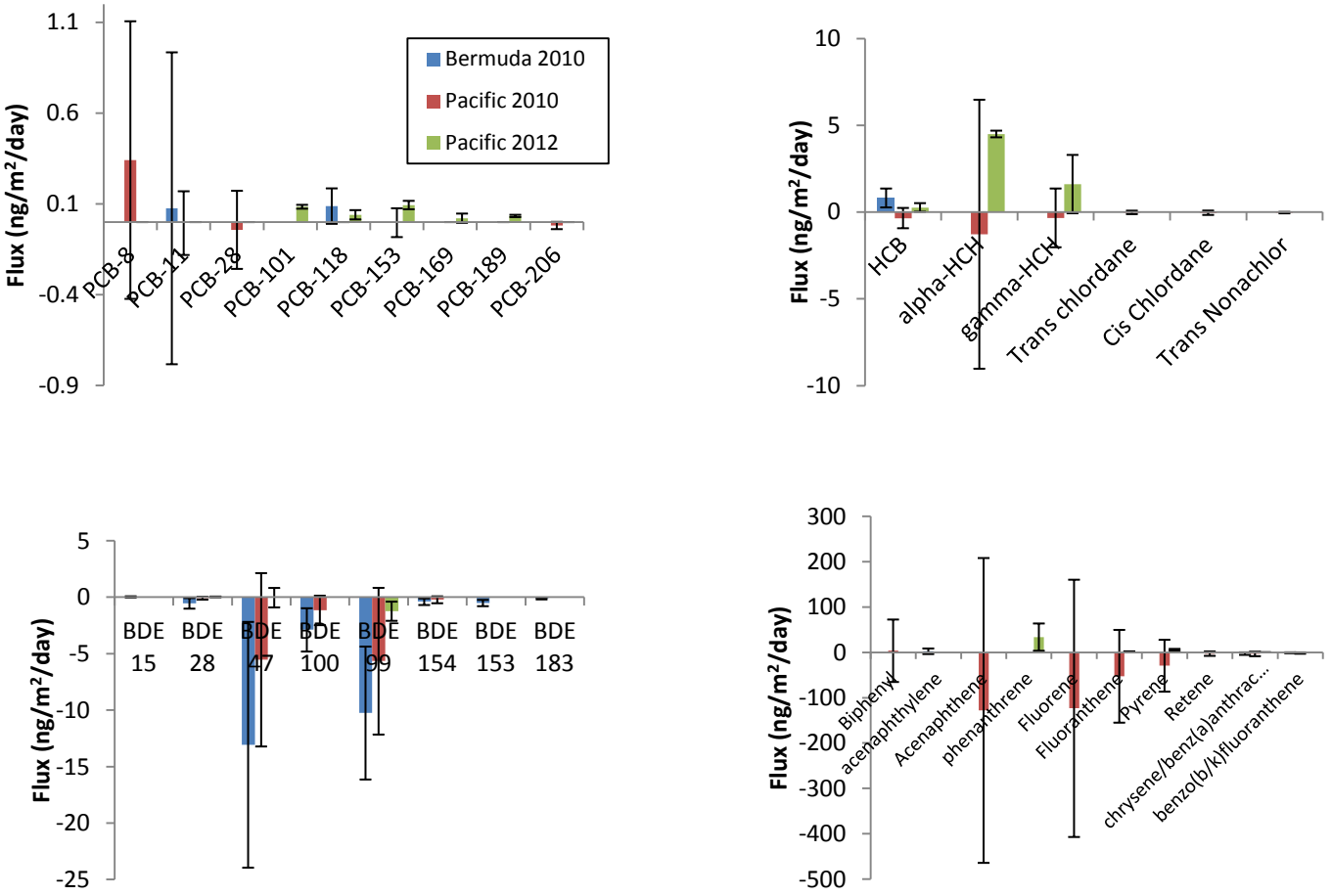

Figure S7. Averaged air-water exchange fluxes of PCBs, OCPs, BDEs and PAHs from the three cruises.

Error bars represent standards deviation between samples from each cruise.

Table S16. Comparison of air and water POPs in the Atlantic Basin and Pacific Basin.

	mean		standard deviation		p-value
	Bermuda (n=4)	Pacific (n=4)	Bermuda (n=4)	Pacific (n=4)	
air samples					
PCB-11	53.67	3.45	18.81	2.73	0.03
hexachlorobenzene	186.20	341.52	38.30	155.01	0.06
BDE-47	114.31	21.99	75.30	13.44	0.03
benzo(b/k)fluoranthene	28.43	12.20	8.33	8.53	0.11
∑PCB	54.4	22.1	18.8	16.2	0.06
∑OCP	186.2	374.7	38.3	156.3	0.03
∑BDE	193.4	41.6	116.8	23.6	0.03
∑PAH	280.0	5149.5	206.0	4985.4	0.11
water samples					
PCB-11	6.99	0.93	4.98	0.68	0.03
hexachlorobenzene	12.60	12.22	5.03	2.43	0.89
BDE-47	31.29	3.52	24.53	2.48	0.03
benzo(b/k)fluoranthene	29.04	5.98	24.92	2.02	0.06
∑PCB	8.3	7.4	4.5	6.9	0.69
∑OCP	12.6	140.3	5.0	66.7	0.03
∑BDE	61.6	4.6	50.0	2.7	0.03
∑PAH	110.4	1249.1	66.7	934.5	0.06
fluxes					
PCB	0.16	0.27	0.83	1.18	0.69
OCP	0.81	-2.08	0.54	6.64	0.34
BDE	-27.7	-12.6	19.6	15.9	0.20
PAH	-0.93	-343	8.95	860	0.69

Table S17. Air-water exchange gradients from the Pacific Cruise (2012).

Compound	Sample				
	A/W-1	A/W-2	A/W-3	A/W-4	A/W-5
PCB-101	25.67667	26.2215	59.21968	11.02049	17.39046
PCB-118	2.868367	34.01495	13.38936	2.067239	2.628154
PCB-153	11.83182	32.58394	134.7381	14.43009	15.77456
PCB-169	9.159632	9.358415	0.973891	5.351974	1.408394
PCB-189	45.64777	23.79258	52.71141	44.19942	159.6471
HCB	0.945115	1.642747	1.062262	1.751578	1.1281
Alpha-HCH	3.519811	9.787344	7.504735	5.289501	0.569672
Gamma-HCH	10.65443	7.663816	0.911488	2.852572	0.835478
BDE 28	494.5424	0.83961	5.015916	5.693202	0.310303
BDE 47	694.4696	0.243868	6.863165	2.438927	7.321813
BDE 99	520.3449	0.036371	0.023571	0.179343	0.028547
Phn	6.524163	3.336509	4.417646	7.467447	2.979941
Fla	8.768237	4.521622	5.314285	14.59396	2.254077
Pyr	26.77355	11.30354	11.11173	25.30162	3.49444
Chr/BaA	7.531307	7.416494	4.261325	0.694419	0.144733

* Colored tables represent significant gradients from equilibrium. orange: evaporation; blue: deposition. Applies to the following tables.

Table S17. Cont'd. Air-water exchange gradients from the Pacific Cruise (2010).

Compound	Sample			
	A/W-1	A/W-2	A/W-3	A/W-4
PCB-8	2.334386	1.219369	17.76452	0.426138
PCB-11	2.519892	0.916958	10.70876	0.193734
PCB-28	1.857686	1.513681	32.65712	0.034314
PCB-153	6.474734	2.002543	110.9164	0.041057
PCB-206	0.249477	0.418183	0.974745	0.43843
HCB	1.674784	0.742008	0.681736	0.7729
alpha-HCH	0.29536	0.770865	0.199538	2.105195
gamma-HCH	5.248379	0.224119	0.209088	0.160941
Trans chlordane	1.643445	0.861786	2.870761	0.389509
Cis Chlordane	0.078616	0.067076	11.07666	0.325903
Trans Nonachlor	1.014579	0.054825	0.087964	0.036656
BDE 28	0.60632	0.206544	1.882568	0.030839
BDE 47	0.251625	0.035343	0.047538	0.010612
BDE 100	0.013018	0.001112	0.016091	0.000801
BDE 99	0.02626	0.006628	0.003958	0.001728
BDE 154	0.018016	0.003321	0.071518	0.001582
Biph	1.33669	2.36027	182.6086	0.009441
Ace	0.410002	0.69913	16.09954	0.043884
Flr	0.79412	1.685817	20.14988	0.01003
Fla	0.297224	0.300542	1.029918	0.016236
Pyr	0.654463	0.553451	2.219351	0.00777
Ret	0.405436	0.113958	0.064716	0.002538
Chr/BaA	0.254972	0.253145	0.325717	0.031634
B(b/k)f	0.252001	0.063219	0.005728	0.003193

Table S17. Cont'd. Air-water exchange gradients from the Atlantic Cruise (2010).

Compound	Sample			
	A/W-1	A/W-2	A/W-3	A/W-4
PCB-11	0.472032	4.993862	0.753676	0.46763
PCB-118	48.83333	3.450847	1.763304	6.847984
HCB	3.559594	3.542354	1.596582	1.418975
BDE 15	0.872176	10.72802	0.362262	3.28632
BDE 28	0.156613	0.689216	0.267278	0.115306
BDE 47	0.200046	0.361862	0.212441	0.021472
BDE 100	0.122859	0.115782	0.046833	0.006064
BDE 99	0.183561	0.18683	0.052542	0.029238
BDE 154	0.134444	0.054301	0.144228	0.004982
BDE 153	0.145373	0.106284	0.068942	0.020951
BDE 183	0.12937	0.186502	0.076656	0.00851
Acy	3.398646	2.311329	0.78902	0.91
Chr/BaA	1.524976	0.645389	0.166934	0.111121
B(b/k)f	0.074967	0.505639	0.029482	0.020761

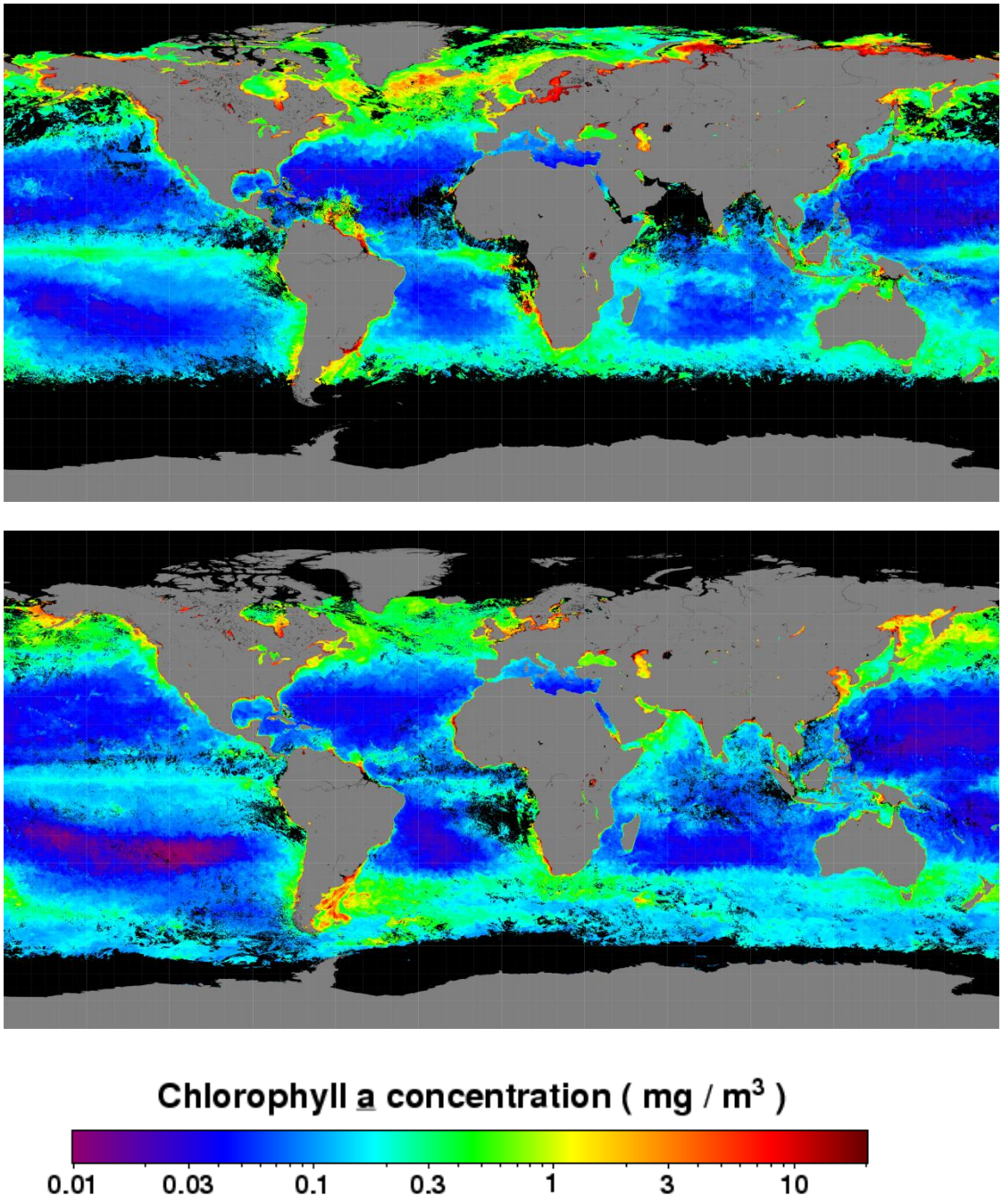

Figure S9. NASA Moderate Resolution Imaging Spectroradiometer (MODIS) sub-surface chlorophyll-a concentration map (top: Jun 2010; bottom: Oct 2012). (Accessed on Sep 14 th, 2015)

BIBLIOGRAPHY

AM, A.-A. (1999). Organochlorine contaminants in microlayer and subsurface water of Alexandria Coast, Egypt. *J AOAC Int*, *82*, J AOAC Int.

Appen, W.-J. Von, Schauer, U., Cabrillo, R. S., Bauerfeind, E., & Beszczynska-Möller, A. (2015). Exchange of warming deep waters across Fram Strait. *Deep Sea Research Part I: Oceanographic Research Papers*, *103*, 86–100. doi:10.1016/j.dsr.2015.06.003

ATSDR. (1997). Toxicological profile for HCB. US Department of Health and Human Services, Public Health Service, Agency for Toxic Substances and Disease Registry (ATSDR). Atlanta, GA.

Baek, S. Y., Jurng, J., & Chang, Y. S. (2013). Spatial distribution of polychlorinated biphenyls, organochlorine pesticides, and dechlorane plus in Northeast Asia. *Atmospheric Environment*, *64*, 40–46. doi:10.1016/j.atmosenv.2012.09.015

Barber, J. L., Sweetman, A. J., Van Wijk, D., & Jones, K. C. (2005). Hexachlorobenzene in the global environment: Emissions, levels, distribution, trends and processes. *Science of the Total Environment*, *349*(1-3), 1–44. doi:10.1016/j.scitotenv.2005.03.014

Bartkow, M. E., Hawker, D. W., Kennedy, K. E., & Müller, J. F. (2004). Characterizing Uptake Kinetics of PAHs from the Air Using Polyethylene-Based Passive Air Samplers of Multiple Surface Area-to-Volume Ratios. *Environmental Science and Technology*, *38*(9), 2701–2706. doi:10.1021/es0348849

Berrojalbiz, N., Dachs, J., Del Vento, S., Ojeda, M. J., Valle, M. C., Castro-Jiménez, J., … Hanke, G. (2011). Persistent organic pollutants in mediterranean seawater and processes affecting their accumulation in plankton. *Environmental Science and Technology*, *45*(10), 4315–4322. doi:10.1021/es103742w

Booij, K., Bommel, R. Van, Aken, H. M. Van, Haren, H. Van, Brummer, G. A., & Ridderinkhof, H. (2014). Passive sampling of nonpolar contaminants at three deep-ocean sites. *Environmental Pollution*, *195*, 101–108.

Booij, K., & Smedes, F. (2010). An improved method for estimating in situ sampling rates of nonpolar passive samplers. *Environmental Science and Technology*, *44*(17), 6789–6794. doi:10.1021/es101321v

Booij, K., Smedes, F., & Van Weerlee, E. M. (2002). Spiking of performance reference compounds in low density polyethylene and silicone passive water samplers. *Chemosphere*, *46*, 1157–1161. doi:10.1016/S0045-6535(01)00200-4

Booij, K., van Bommel, R., Jones, K.C., Barber, J. L. (2007). Air-water distribution of hexachlorobenzene and 4,40-DDE along a North-South Atlantic transect. *Marine Pollution Bulletin*, *54*(6), 814–819. doi:10.1016/j.marpolbul.2006.12.015

Bullister, J. (2014). Atmospheric CFC-11, CFC-12, CFC-113, CCl4 and SF6 Histories (1910-2014). Retrieved June 10, 2015, from http://cdiac.ornl.gov/oceans/new_atmCFC.html

D. S. Mackay, W. Y. Wan, K. C. Ma, S. C. L. (2006). *Physical-Chemical Properties and Environmental Fate for Organic Chemicals*. Florida, USA: CRC Press, Taylor & Francis Group.

Ding, X., Wang, X. M., Xie, Z. Q., Xiang, C. H., Mai, B. X., Sun, L. G., … Fu, J. M. (2007). Atmospheric hexachlorocyclohexanes in the North Pacific Ocean and the adjacent Arctic region: Spatial patterns, chiral signatures, and sea-air exchanges. *Environmental Science and Technology*, *41*(15), 5204–5209. doi:10.1021/es070237w

E.Q.Pilson, M. (2013). *An introduction to the chemistry of the sea* (2nd ed.).

Gioia, R., Dachs, J., Nizzetto, L., Lohmann, R., Jones, K. C., & Girona, C. J. (2013). Atmospheric Transport , Cycling and Dynamics of Polychlorinated Biphenyls (PCBs) from. In *Occurrence, Fate and Impact of Atmospheric Poluutants on Environmental and Human Health* (pp. 1–18). Washington DC.

Gioia, R., Lohmann, R., Dachs, J., Temme, C., Lakaschus, S., Schulz-Bull, D., … Jones, K. C. (2008a). Polychlorinated biphenyls in air and water of the North Atlantic and Arctic Ocean. *Journal of Geophysical Research*, *113*(D19), D19302. doi:10.1029/2007JD009750

Gioia, R., Nizzetto, L., Lohmann, R., Dachs, J., Temme, C., & Jones, K. C. (2008b). Polychlorinated Biphenyls (PCBs) in Air and Seawater of the Atlantic Ocean: Sources, Trends and Processes. *Environmental Science & Technology*, *42*(5), 1416–1422. doi:10.1021/es071432d

González-Gaya, B., Dachs, J., Roscales, J. L., Caballero, G., & Jiménez, B. (2014). Perfluoroalkylated Substances in the Global Tropical and Subtropical Surface Oceans. *Environmental Science & Technology*, *48*(22), 13076–13084. doi:10.1021/es503490z

Harner, T., Kylin, H., Bidleman, T. F., Strachan, W. M. J. (1999). Removal of alpha- and gamma-hexachlorocyclohexane and enantiomers of alpha-hexachlorocyclohexane in the eastern Arctic Ocean. *Environmental Science & Technology*, *33*, 1157–1164.

Iwata, H., Tanabe, S., Sakai, N., & Tatsukawa, R. (1993). Distribution of Persistent Organochlorines in the Oceanic Air and Surface Seawater and the Role of Ocean on Their Global Transport and Fate. *Environmental Science and Technology*, *27*(6), 1080–1098. doi:10.1021/es00043a007

Jantunen, L. M., Helm, P. A., Kylin, H., and Bidlemant, T. F. (2008). Hexachlorocyclohexanes (HCHs) in the Canadian archipelago. 2. Air-water gas exchange of alpha- and gamma-HCH. *Environ. Sci. Technol*, *42*, 465–470.

Jones, K. C., Barber, J. L., Booij, K., & Jaward, F. M. (2004). Evidence for dynamic air-water coupling of persistent organic pollutants over the open Atlantic Ocean. *Environmental Science and Technology*, *38*, 2617–2625. doi:10.1021/es049881q

Kallenborn, R., Christensen, G., Evenset, A., Schlabach, M., & Stohl, A. (2007). Atmospheric transport of persistent organic pollutants (POPs) to Bjørnøya (Bear island). *Journal of Environmental Monitoring : JEM*, *9*(10), 1082–1091. doi:10.1039/b707757m

Khairy, M. a, & Lohmann, R. (2014). Field calibration of low density polyethylene passive samplers for gaseous POPs. *Environmental Science. Processes & Impacts*, *16*, 414–21. doi:10.1039/c3em00493g

Khairy, M. a., & Lohmann, R. (2013). Feasibility of using low density polyethylene sheets to detect atmospheric organochlorine pesticides in Alexandria, Egypt. *Environmental Pollution*, *181*, 151–158. doi:10.1016/j.envpol.2013.06.031

Knauss, J. A. (2005). *Introduction to physical oceanography* (2nd ed.). Waveland Press, Inc.

Komp, P., & McLachlan, M. S. (1997). Octanol/air partitioning of polychlorinated biphenyls. *Environmental Toxicology and Chemistry*, *16*(12), 2433–2437. doi:10.1002/etc.5620161201

Lohmann, R. (2012a). A critical review of low-density polyethylene's partitioning and diffusion coefficients for trace organic contaminants and implications for its use as a passive sampler. *Environmental Science and Technology*, *46*, 606–618.

Lohmann, R., Gioia, R., Jones, K. C., Nizzetto, L., Temme, C., Xie, Z., … Jantunen, L. (2009). Organochlorine pesticides and PAHs in the surface water and atmosphere of the North Atlantic and Arctic Ocean. *Environmental Science and Technology*, *43*(15), 5633–5639. doi:10.1021/es901229k

Lohmann, R., Klanova, J., Kukucka, P., Yonis, S., & Bollinger, K. (2012b). PCBs and OCPs on a east-to-west transect: The importance of major currents and net volatilization for PCBs in the atlantic ocean. *Environmental Science and Technology*, *46*, 10471–10479. doi:10.1021/es203459e

Lohmann, R., Klanova, J., Kukucka, P., Yonis, S., & Bollinger, K. (2013a). Concentrations, fluxes, and residence time of PBDEs across the tropical Atlantic Ocean. *Environmental Science and Technology*, *47*, 13967–13975. doi:10.1021/es403494b

Lohmann, R., Klanova, J., Pribylova, P., Liskova, H., Yonis, S., & Bollinger, K. (2013). PAHs on a west-to-east transect across the tropical Atlantic Ocean. *Environmental Science and Technology*, *47*(6), 2570–2578. doi:10.1021/es304764e

Lohmann, R., & Muir, D. (2010). Global aquatic passive sampling (AQUA-GAPS): Using passive samplers to monitor POPs in the waters of the world. *Environmental Science and Technology*, *44*(3), 860–864. doi:10.1021/es902379g

Ma, Y. G., Lei, Y. D., Xiao, H., Wania, F., & Wang, W. H. (2010). Critical review and recommended values for the physical-chemical property data of 15 polycyclic aromatic hydrocarbons at 25 ??C. *Journal of Chemical and Engineering Data*, *55*(2), 819–825. doi:10.1021/je900477x

Ma, Y., Xie, Z., Yang, H., Möller, A., Halsall, C., Cai, M., … Ebinghaus, R. (2013). Deposition of polycyclic aromatic hydrocarbons in the North Pacific and the Arctic. *Journal of Geophysical Research: Atmospheres*, *118*(2004), 5822–5829. doi:10.1002/jgrd.50473

Martí, S., Bayona, J. M., & Albaigés, J. (2001). A Potential Source of Organic Pollutants into the Northeastern Atlantic: The Outflow of the Mediterranean Deep-Lying Waters through the Gibraltar Strait. *Environmental Science & Technology*, *35*(13), 2682–2689. doi:10.1021/es000258p

Möller, A., Xie, Z., Cai, M., Zhong, G., Huang, P., Cai, M., … Ebinghaus, R. (2011a). Polybrominated diphenyl ethers vs alternate brominated flame retardants and dechloranes from East Asia to the arctic. *Environmental Science and Technology*, *45*(16), 6793–6799. doi:10.1021/es201850n

Möller, A., Xie, Z., Sturm, R., & Ebinghaus, R. (2011b). Polybrominated diphenyl ethers (PBDEs) and alternative brominated flame retardants in air and seawater of the European Arctic. *Environmental Pollution*, *159*(6), 1577–1583. doi:10.1016/j.envpol.2011.02.054

Murayama H, Takase Y, Mitobe H, Mukai H, Ohzeki T, Shimizu K, et al. (2003). Seasonal changes of persistent organic pollutant concen- trations in air at Niigata area, Japan. *Chemosphere*, *52*, 683–94.

Nizzetto, L., Lohmann, R., Gioia, R., Jahnke, A., Temme, C., Dachs, J., … Jones, K. C. (2008). PAHs in Air and Seawater along a North–South Atlantic Transect:

Trends, Processes and Possible Sources. *Environmental Science & Technology*, *42*(5), 1580–1585. doi:10.1021/es0717414

Rene P. Schwarzenbach, Philip M. Gschwend, D. M. I. (2002). *Environmental Organic Chemistry*. (2nd, Ed.). Wiley Interscience.

Renee L. Falconer, T. F. B. (1994). Vapor pressures and predicted particle/gas distributions of polychlorinated biphenyl congeners as functions of temperature and ortho-chlorine substitution. *Atmospheric Environment*, *28*, 547–554.

Ruge, Z. (2013). Air-water exchange and trends of persistent bioaccumulative toxics (PBTs) across Lake Superior. Master's Thesis.

Schauer, U., Fahrbach, E., Osterhus, S., & Rohardt, G. (2004). Arctic warming through the Fram Strait: Oceanic heat transport from 3 years of measurements. *Journal of Geophysical Research C: Oceans*, *109*(6), 1–14. doi:10.1029/2003JC001823

Schenker, U., Macleod, M., Scheringer, M., & Hungerbühler, K. (2005). Improving Data Quality for Environmental Fate Models: A Least-Squares Adjustment Procedure for Harmonizing Physicochemical Properties of Organic Compounds. *Environmental Science and Technology*, *39*(8), 8434–8441.

Schulz, D. E., Petrick, G., & Duinker, J. C. (1988). Chlorinated biphenyls in North Atlantic surface and deep water. *Marine Pollution Bulletin*, *19*(10), 526–531. doi:10.1016/0025-326X(88)90543-7

Schulz-Bull, D. E., Petrick, G., Bruhn, R., & Duinker, J. C. (1998). Chlorobiphenyls (PCB) and PAHs in water masses of the northern North Atlantic. *Marine Chemistry*, *61*(1-2), 101–114. doi:10.1016/S0304-4203(98)00010-3

Sobek, A., & Gustafsson, O. (2004). Latitudinal fractionation of polychlorinated biphenyls in surface seawater along a 62 degrees N-89 degrees N transect from the southern Norwegian Sea to the North Pole area. *Environmental Science and Technology*, *38*(10), 2746–2751. doi:10.1021/es0353816

Sobek, A., & Gustafsson, Ö. (2014). Deep water masses and sediments are main compartments for polychlorinated biphenyls in the Arctic Ocean. *Environmental Science and Technology*, *48*(12), 6719–6725. doi:10.1021/es500736q

Strachan WMJ, Fisk A, Teixeira CF, Burnsiton DA, N. R. (n.d.). PCBs and organochlorine pesticide concentrations in the waters of the Canadian Archipelago and other Arctic regions (Abstract 13). In *Proceedings of the Workshop on persistent organic pollutants (POPs) in the Arctic: Human health and environmental concerns.* Arctic Monitoring and Assessment Program: Rovaniemi Finland, 2000: AMAP report.

Tittlemier, S. a, Halldorson, T., Stern, G. a, & Tomy, G. T. (2002). Vapor pressures, aqueous solubilities, and Henry's law constants of some brominated flame retardants. *Environmental Toxicology and Chemistry / SETAC*, *21*(9), 1804–1810. doi:10.1002/etc.5620210907

Tukey, J. (1977). Exploratory data analysis. *Addison-Wesely*.

Wania, F., & Dugani, C. B. (2003). Assessing the long-range transport potential of polybrominated diphenyl ethers: a comparison of four multimedia models. *Environmental Toxicology and Chemistry / SETAC*, *22*(6), 1252–1261. doi:10.1897/1551-5028(2003)022<1252:atlrtp>2.0.co;2

Wong, F., & Wong, F. (2010). *Air-surface Exchange of Persistent Organic Pollutants in North America*. University of Toronto.

Wu, X., Lam, J. C. W., Xia, C., Kang, H., Sun, L., Xie, Z., & Lam, P. K. S. (2010). Atmospheric HCH concentrations over the marine boundary layer from Shanghai, China to the arctic ocean: Role of human activity and climate change. *Environmental Science and Technology*, *44*(22), 8422–8428. doi:10.1021/es102127h

Xie, Z., Koch, B. P., Möller, a., Sturm, R., & Ebinghaus, R. (2011). Transport and fate of hexachlorocyclohexanes in the oceanic air and surface seawater. *Biogeosciences*, *8*(9), 2621–2633. doi:10.5194/bg-8-2621-2011

Xie, Z., Möller, A., Ahrens, L., Sturm, R., & Ebinghaus, R. (2011). Brominated flame retardants in seawater and atmosphere of the Atlantic and the southern ocean. *Environmental Science and Technology*, *45*(5), 1820–1826. doi:10.1021/es103803t

Zhang, L., Bidleman, T., Perry, M. J., & Lohmann, R. (2012). Fate of chiral and achiral organochlorine pesticides in the north Atlantic bloom experiment. *Environmental Science and Technology*, *46*, 8106–8114. doi:10.1021/es3009248

Zhang, L., & Lohmann, R. (2010). Cycling of PCBs and HCB in the surface ocean-lower atmosphere of the open pacific. *Environmental Science and Technology*, *44*(10), 3832–3838. doi:10.1021/es9039852